Annals of Physics 327 (2012) 1408–1433

Contents lists available at SciVerse ScienceDirect

Annals of Physics

journal homepage: www.elsevier.com/locate/aop

A quantum photonic dissipative transport theory

Chan U Lei [a], Wei-Min Zhang [b,*]

[a] Department of Physics, California Institute of Technology, Pasadena, CA 91125, USA

[b] Department of Physics and Center for Quantum Information Science, National Cheng Kung University, Tainan 70101, Taiwan

ARTICLE INFO

Article history:
Received 29 September 2011
Accepted 13 February 2012
Available online 20 February 2012

Keywords:
Quantum photonic transport
Photonic crystals
Photonic integrated circuits
Open quantum systems and quantum dissipation dynamics
Feynman–Vernon influence functional theory
Nonequilibrium Green function approach

ABSTRACT

In this paper, a quantum transport theory for describing photonic dissipative transport dynamics in nanophotonics is developed. The nanophotonic devices concerned in this paper consist of on-chip all-optical integrated circuits incorporating photonic bandgap waveguides and driven resonators embedded in nanostructured photonic crystals. The photonic transport through waveguides is entirely determined from the exact master equation of the driven resonators, which is obtained by explicitly eliminating all the degrees of freedom of the waveguides (treated as reservoirs). Back-reactions from the reservoirs are fully taken into account. The relation between the driven photonic dynamics and photocurrents is obtained explicitly. The non-Markovian memory structure and quantum decoherence dynamics in photonic transport can then be fully addressed. As an illustration, the theory is utilized to study the transport dynamics of a photonic transistor consisting of a nanocavity coupled to two waveguides in photonic crystals. The controllability of photonic transport through the external driven field is demonstrated.

1. Introduction

With the rapid development of nanotechnology, all-optical photonic circuits embedded in nanoscale photonic crystals have received tremendous attention [1,2]. The on-chip all-optical integrated circuits are considered as the promising nanophotonic devices for robust interconnect networks used in optical communication. Photonic crystals are artificial nanomaterials with periodic refractive index. The photonic band gap (PBG) structures together with characteristic dispersion properties make the light manipulation and transmission much more efficient. For examples, strong light

* Corresponding author. Tel.: +885 62757575; fax: +886 62747995.
E-mail address: wzhang@mail.ncku.edu.tw (W.-M. Zhang).

0003-4916/$ – see front matter © 2012 Elsevier Inc. All rights reserved.
doi:10.1016/j.aop.2012.02.005

confinement can be realized by introducing point defect (nanocavity) in photonic crystals [3], slow lights can be generated by waveguide structures with controllable dispersion properties, which can be implemented by introducing line defects or series of coupled point defects in photonic crystals [4,5]. Various novel nanophotonic devices have been constructed or proposed by the combinations of different defects with PBG structures, such as optical switches [6], filters [7], memory devices [8] and on-chip single photon guns [9]. Furthermore, with the new development of the semiconductor nanofabrication techniques, many tunable functional nanophotonic devices have also been proposed and modeled recently. Different techniques are utilized to characterize various physical properties in these nanophotonic devices. In particular, properties such as the resonance frequency of a nanoresonator or the band structure of a waveguide can be tuned by changing the refractive index of the photonic crystal through thermooptic effect [10], electrooptical effect [11], fluid insertion [12], or even by mechanically changing the structure of the photonic crystal [13]. Couplings between different elements in a photonic circuit can be controlled by nanoelectromechanical systems [14]. These dynamical tunable nanodevices greatly expand their applications in photonic integrated circuitry and further stimulate the potential application in quantum information processing.

To achieve the goal of quantum information processing in terms of all-optical processing, information carriers should be individual photons. Photonic transmission processes in nanophotonics should be performed in an ultrafast and well-controllable way. In such a situation, the nanophotonic devices are far away from equilibrium, then the non-Markovian memory and quantum decoherence dynamics dominate the photonic transport. Thus, a fundamental quantum transport theory that can incorporate with the non-Markovian memory structure and quantum decoherence dynamics for photonic transmission is highly demanded.

In fact, non-Markovian dynamics in quantum optics has been extensively studied for a few-level atom placed inside photonic crystals [15,16]. The typical features of the non-Markovian dynamics include atomic population trapping (inhibition of spontaneous emission), strong localization of light, formulation of atom–photon bound states, and collective switching behavior in the vicinity of the PBG [17–21]. These features can be determined exactly from the Schrödinger equation of an atomic-photon state contains only a single photon, or using a perturbative expansion to the Heisenberg equation of motion in the weak coupling limit of the atom-field interacting with the reservoir. When the number of photon increases or the perturbation break down, the problem becomes intractable. The general non-Markovian dynamics involving arbitrary number of photons at arbitrary temperature for a structured reservoir has not been fully understood. Recently, we have utilized the exact master equation of a micro/nano cavity coupled to a general thermal reservoir or a structured reservoir in photonic crystals to study non-perturbatively various non-Markovian processes involving arbitrary number of photons at an arbitrary temperature [22,23]. However, a quantum photonic transport theory describing photonic transmission dynamics in all-optical nanophotonic circuits has not yet been established.

A fundamental quantum transport theory should be treated in a fully nonequilibrium way. Modern nonequilibrium physics was developed based on the Schwinger–Keldysh nonequilibrium Green function technique [24,25] and the Feynman–Vernon influence functional approach [26]. The nonequilibrium Green function technique allows a systematic perturbative [27] and also a non-perturbative [28] study for various nonequilibrium phenomena in many-body electronic systems. It has become a very powerful tool in the study of quantum electron transport in mesoscopic physics [29]. However, such an approach has not been utilized to investigate photonic transport in all-optical processing. Besides, the non-Markovian memory structure and the quantum decoherence dynamics have not been well explored in terms of the nonequilibrium Green functions in the transient quantum transport. On the other hand, the Feynman–Vernon influence functional approach [26] has been widely used to study the dissipation dynamics in quantum tunneling problems [30] and the decoherence dynamics in quantum measurement theory [31]. It is particularly useful in the derivation of the exact master equation for the quantum Brownian motion (QBM), achieved by completely integrating out the environmental degrees of freedom through the functional integral [32,33]. The QBM is modeled as a central harmonic oscillator linearly coupled to a thermal bath simulated by a set of harmonic oscillators. Applications of the QBM exact master equation cover various topics, such as quantum decoherence, quantum-to-classical transition, and quantum measurement theory,

etc. [34,35]. However, there are very few applications of such a master equation approach to the quantum transport dynamics. Typical examples are the real-time diagrammatic expansion [36] and the hierarchical equations-of-motion expansion [37]. A closed formulation for the transient electron transport in nanoelectronics has just been established very recently by one of us through the use of the Feynman–Vernon influence functional approach [38,39].

In this paper, we shall present a quantum transport theory to depict photonic transport for on-chip all-optical nanophotonics. We will focus on the dynamics of photonic transport between the resonators and the waveguides through the controllable photonic dynamics of the driven resonators. The photonic dynamics of the driven resonators is determined by the exact master equation where the waveguides are treated as reservoirs. The back-reactions between the waveguides and the resonators, i.e. the non-Markovian dissipation and fluctuation induced from the back-reactions of the waveguides, are fully taken into account through the use of the Feynman–Vernon influence functional approach. The exact master equation for nanophotonics is derived nonperturbatively. The photocurrents that describe the transient photonic transport are then obtained directly from the master equation. The full responses of the photonic transport under the control of external driving fields are presented explicitly.

The remainder of the paper is organized as follows. In Section 2, we model nanophotonic devices in terms of an open optical system in general, and specify them in nanostructured photonic crystals in particular. The fundamental Hamiltonian for the nanophotonic devices is derived from first-principle. The derivation of the exact master equation for the driven resonators is presented in Section 3, where the responses of the resonator dynamics to the external driving field are given explicitly. In Section 4, the photonic transport theory is established. The photocurrents flowing from the resonators into individual waveguides that describe the photonic transport in the circuit are derived from the exact master equation. The non-Markovian memory structure and the quantum decoherence dynamics in the transport processes can then be explored explicitly. A comparison of the present theory with the electron transport in mesoscopic systems based on Keldysh's nonequilibrium Green function technique is also presented, from which the generalized nonequilibrium lesser (correlation) Green function, which determines the nonequilibrium quantum kinetics completely, is solved. In Section 4, the present theory is utilized to investigate quantum transport dynamics in a photonic transistor consisting of a driving nanocavity coupled to two waveguides in photonic crystals, as an illustration. The controllability of the photocurrent through the photonic transistor is analytically and numerically analyzed. Finally, a summary is presented in Section 5.

2. On-chip all-optical photonic nanodevices

The on-chip all-optical nanophotonic devices considered in this paper consist of photonic band gap structure incorporating with cavities and waveguides whose spectra lie within the band gap of the photonic crystal, as shown in Fig. 1. For the sake of simplicity, we restrict ourselves to photonic crystals made up of a linear, isotropic and transparent medium. Thus, the photonic device can be characterized by a real scalar dielectric constant $\epsilon(\mathbf{r})$ which is explicitly spatial dependent [1]. To quantize the fields in photonic devices in terms of the cavities and the waveguides modes, we adopt the system–reservoir quantization formalism of a generalized canonical quantization to the electromagnetic field in medium [40,41]. The electric and magnetic fields in the photonic devices can be expressed in terms of the vector potential $\mathbf{A}(\mathbf{r}, t)$ and a scalar potential $\phi(\mathbf{r})$:

$$\mathbf{E} = -\nabla\phi - \frac{1}{c}\frac{\partial \mathbf{A}}{\partial t}, \qquad \mathbf{B} = \nabla \times \mathbf{A}. \tag{1}$$

We shall work in the Coulomb gauge and in the absence of source, which corresponds to the choice of $\phi = 0$ with the transversality condition $\nabla \cdot [\epsilon(\mathbf{r})\mathbf{A}(\mathbf{r}, t)] = 0$. Then the Hamiltonian of the electromagnetic field for photonic devices is given by

$$H = \frac{1}{2}\int d^3\mathbf{r}\Big[\frac{c^2\mathbf{\Pi}(\mathbf{r}, t)^2}{\epsilon(\mathbf{r})} + (\nabla \times \mathbf{A}(\mathbf{r}, t))^2\Big], \tag{2}$$

where $\mathbf{\Pi}(\mathbf{r}, t) = \epsilon(\mathbf{r})\dot{\mathbf{A}}(\mathbf{r}, t)/c^2$ is the canonical conjugate of the vector potential $\mathbf{A}(\mathbf{r}, t)$.

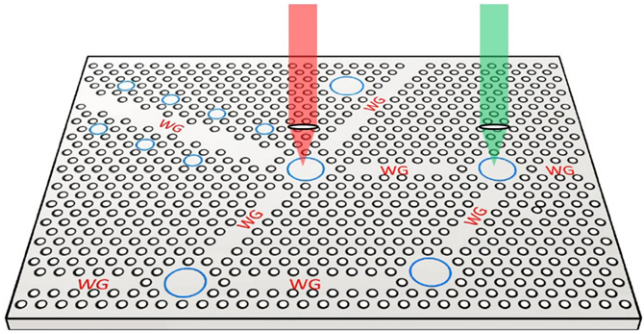

Fig. 1. A schematic diagram of all-optical photonic devices incorporating photonic bandgap waveguides and resonators with external driving fields in nanostructured photonic crystals.

The vector potential can be expended in terms of a complete set of mode functions, $\{\mathbf{f}_k(\mathbf{r})\}$, which are determined by the wave equation

$$\nabla \times [\nabla \times \mathbf{f}_k(\mathbf{r})] - \frac{\epsilon(\mathbf{r})\omega_k^2}{c^2}\mathbf{f}_k(\mathbf{r}) = \mathbf{0}, \tag{3}$$

where the mode functions satisfy the orthonormality condition

$$\int d^3\mathbf{r}\epsilon(\mathbf{r})\mathbf{f}_k^*(\mathbf{r}) \cdot \mathbf{f}_{k'}(\mathbf{r}) = \delta_{k,k'}. \tag{4}$$

Utilizing the Feshbach projection technique [42], we separate the whole space of the photonic crystal by the region $\Im_i$ occupied by the cavity i, the region $\Im_\alpha$ occupied by the waveguides α and the region left denoted by $\Im_b$ as the background photonic crystal structure. Because of the presence of the PBG structure, the micro/nano cavities in photonic crystals have a very high Q factor, and the photon lost into the photonic crystal is also extremely low. Thus the field in $\Im_b$ is negligible, as an advantage of lossless materials for photonic crystals [1,2]. Consequently, the exact eigenmodes of the vector potential in the photonic circuit can be decomposed into the eigenmodes in the regions $\Im_i$ and $\Im_\alpha$, respectively

$$\mathbf{f}_k(\mathbf{r}) = \sum_i \alpha_i^k \mathbf{u}_i(\mathbf{r}) + \sum_\alpha \sum_{k'} \beta_{\alpha k'}^k \mathbf{v}_{\alpha k'}(\mathbf{r}), \tag{5}$$

where $\mathbf{u}_i(\mathbf{r})$ is the eigenmode of the cavity i, $\mathbf{v}_{\alpha k}(\mathbf{r})$ is the continuum eigenmode of the waveguide α. Both of them form a complete and orthonormal basis set in the regions $\Im_i$ and $\Im_\alpha$ separately, while α_i^k and β_α^k are the expansion coefficients. The eigenmodes of the cavities and the waveguides satisfy the following equations with the boundary conditions [40]:

$$\nabla \times [\nabla \times \mathbf{u}_i(\mathbf{r})] - \frac{\epsilon(\mathbf{r})\omega_i^2}{c^2}\mathbf{u}_i(\mathbf{r}) = \mathbf{0}, \qquad \mathbf{n} \times [\nabla \times \mathbf{u}_i(\mathbf{r})]\,|_{\partial\Im_i} = \mathbf{0}; \tag{6a}$$

$$\nabla \times [\nabla \times \mathbf{v}_{\alpha k}(\mathbf{r})] - \frac{\epsilon(\mathbf{r})\omega_{\alpha k}^2}{c^2}\mathbf{v}_{\alpha k}(\mathbf{r}) = \mathbf{0}, \qquad \mathbf{n} \times \mathbf{v}_{\alpha k}(\mathbf{r})\,|_{\partial\Im_\alpha} = \mathbf{0}. \tag{6b}$$

With the above decomposition of the eigenmodes, the vector potential of the electromagnetic field in the photonic device and its canonical conjugate can be expended in terms of the cavities eigenmodes and the continuous modes of the waveguides

$$\begin{aligned} \mathbf{A}(\mathbf{r}, t) &= \sum_i \mathbf{A}_i(\mathbf{r}, t) + \sum_\alpha \mathbf{A}_\alpha(\mathbf{r}, t), \\ \mathbf{\Pi}(\mathbf{r}, t) &= \sum_i \mathbf{\Pi}_i(\mathbf{r}, t) + \sum_\alpha \mathbf{\Pi}_\alpha(\mathbf{r}, t), \end{aligned} \tag{7}$$

where $\mathbf{A}_i(\mathbf{r},t)$, $\mathbf{\Pi}_i(\mathbf{r},t)$ and $\mathbf{A}_\alpha(\mathbf{r},t)$, $\mathbf{\Pi}_\alpha(\mathbf{r},t)$ are vector potentials and their canonical conjugate momenta in the cavity i and the waveguide α, which can be quantized by following the standard quantum field theory in medium. Without the loss of generality and also for simplifying the notation, the photonic circuit being considered consists of N single mode cavities coupling with M waveguides, each waveguide has a single continuous spectrum (it is indeed straightforward to generalize the result to the case of multi-mode cavities). Then we have

$$\mathbf{A}_i(\mathbf{r},t) = c\sqrt{\frac{\hbar}{2\omega_i}}\left[a_i\mathbf{u}_i(\mathbf{r})e^{-i\omega_i t} + a_i^\dagger\mathbf{u}_i^*(\mathbf{r})e^{i\omega_i t}\right], \tag{8a}$$

$$\mathbf{\Pi}_i(\mathbf{r},t) = -\frac{i\epsilon(\mathbf{r})}{c}\sqrt{\frac{\hbar\omega_i}{2}}\left[a_i\mathbf{u}_i(\mathbf{r})e^{-i\omega_i t} - a_i^\dagger\mathbf{u}_i^*(\mathbf{r})e^{i\omega_i t}\right], \tag{8b}$$

$$\mathbf{A}_\alpha(\mathbf{r},t) = c\sum_k\sqrt{\frac{\hbar}{2\omega_k}}\left[c_{\alpha k}\mathbf{v}_{\alpha k}(\mathbf{r})e^{-i\omega_k t} + c_{\alpha k}^\dagger\mathbf{v}_{\alpha k}^*(\mathbf{r})e^{i\omega_k t}\right], \tag{8c}$$

$$\mathbf{\Pi}_\alpha(\mathbf{r},t) = -\frac{i\epsilon(\mathbf{r})}{c}\sum_k\sqrt{\frac{\hbar\omega_k}{2}}\left[c_{\alpha k}\mathbf{v}_{\alpha k}(\mathbf{r})e^{-i\omega_k t} - c_{\alpha k}^\dagger\mathbf{v}_{\alpha k}^*(\mathbf{r})e^{i\omega_k t}\right], \tag{8d}$$

where the operators a_i, $a_i^\dagger$ and $c_{\alpha k}$, $c_{\alpha k}^\dagger$ are the creation and annihilation operators of the fields in the cavity i and the waveguide α. They obey the following commutation relations

$$\begin{aligned}&[a_i, a_j^\dagger] = \delta_{ij}, \qquad [c_{\alpha k}, c_{\alpha' k'}^\dagger] = \delta_{\alpha\alpha'}\delta_{kk'},\\ &[a_i, a_j] = [c_{\alpha k}, c_{\alpha' k'}] = [a_i, c_{\alpha k}] = [a_i^\dagger, c_{\alpha k}] = 0.\end{aligned} \tag{9}$$

Substitute the representations (8) into the Hamiltonian (2), one arrives at the following Hamiltonian for the photonic circuit

$$H = \sum_i\hbar\omega_i a_i^\dagger a_i + \sum_\alpha\sum_k\hbar\omega_k c_{\alpha k}^\dagger c_{\alpha k} + \hbar\sum_i\sum_{\alpha,k}\left[V_{i\alpha k}a_i^\dagger c_{\alpha k} + \widetilde{V}_{i\alpha k}a_i c_{\alpha k} + \text{H.c.}\right], \tag{10}$$

where $V_{i\alpha k}$ and $\widetilde{V}_{i\alpha k}$ are resonant and nonresonant coupling constants between the cavities and the waveguides, and they are determined by

$$V_{i\alpha k} = \frac{c^2}{2\sqrt{\omega_i\omega_k}}\int_{\partial\Im_i\cap\partial\Im_\alpha}[\mathbf{u}_i^*(\mathbf{r})\times\mathbf{n}]\cdot[\nabla\times\mathbf{v}_{\alpha k}(\mathbf{r})], \tag{11a}$$

$$\tilde{V}_{i\alpha k} = \frac{c^2}{2\sqrt{\omega_i\omega_k}}\int_{\partial\Im_i\cap\partial\Im_\alpha}[\mathbf{u}_i(\mathbf{r})\times\mathbf{n}]\cdot[\nabla\times\mathbf{v}_{\alpha k}(\mathbf{r})]. \tag{11b}$$

Here we have ignored the couplings between different cavities, and between different waveguides because their spatial overlaps should be very small. Also, due to the PBG structure in photonic crystals, the features of the high Q-factor micro/nano cavities and the lossless waveguides allow us to neglect the nonresonant terms. Thus, the Hamiltonian of the photonic circuit incorporating M photonic bandgap waveguides and N resonators can be rewritten simply as follows:

$$H = \sum_{i=1}^N\hbar\omega_i a_i^\dagger a_i + \sum_{\alpha=1}^M\sum_k\hbar\omega_{\alpha k}c_{\alpha k}^\dagger c_{\alpha k} + \hbar\sum_i\sum_{\alpha,k}\left(V_{i\alpha k}a_i^\dagger c_{\alpha k} + \text{H.c.}\right). \tag{12}$$

The explicit form of the cavity and waveguide dispersions, ω_i and $\omega_{\alpha k}$, and the coupling between the cavity i and the waveguide α, $V_{i\alpha k}$, depends on the detailed implementation of the photonic circuit in photonic crystals and can be obtained by solving the eigenmode equation (6). It is worth pointing out that the above derivation of the model Hamiltonian can be extended straightforwardly to photonic circuits embedded in other nanophotonic metamaterials.

Furthermore, to control the photonic transport in nanophotonic circuits, we must incorporate the external driving fields applied to the cavities and the waveguides, which can be realized by embedding light emitters such as quantum dot or nanowire to the cavities and the waveguides [7]. Then the Hamiltonian is modified as

$$H(t) = \sum_i \hbar\omega_i a_i^\dagger a_i + \sum_i \left(f_i(t)a_i^\dagger + f_i^*(t)a_i\right) + \sum_{\alpha k} \hbar\omega_{\alpha k} c_{\alpha k}^\dagger c_{\alpha k} + \sum_{\alpha k}\left(f_{\alpha k}(t)c_{\alpha k}^\dagger + f_{\alpha k}^*(t)c_{\alpha k}\right) + \hbar\sum_{i\alpha k}\left(V_{i\alpha k}(t)a_i^\dagger c_{\alpha k} + V_{i\alpha k}^*(t)c_{\alpha k}^\dagger a_i\right). \tag{13}$$

This implementation is quite different from the nanoelectronic transport in mesoscopic systems in nanostructures [29,39]. For the electron transport in mesoscopic systems, such as single electron transistors, one applies bias and gate voltages to the electrodes and the central region to adjust the Fermi surfaces of the electrodes and the energy levels of the central region. Here one has to use the external driving fields directly acting on the photonic device, namely on the cavities and the waveguides, which leads the Hamiltonian to contain additional terms that are explicitly proportional to the external driving fields.

Mathematically, we can transfer the external driving field $f_{\alpha k}(t)$ acting on the waveguide α into an equivalent external field acting on the cavities: $f_i(t) \to \tilde{f}_i(t) = f_i(t) - V_{i\alpha k}(t)f_{\alpha k}(t)/\hbar\omega_{\alpha k}$ through a shift of the waveguide operator $c_{\alpha k} \to \tilde{c}_{\alpha k} = c_{\alpha k} + f_{\alpha k}(t)/\hbar\omega_{\alpha k}$. Thus the general Hamiltonian for nanophotonic circuits can be divided into three parts

$$H(t) = H_S(t) + \sum_\alpha H_{E\alpha} + \sum_\alpha H_{T\alpha}(t), \tag{14}$$

where,

$$H_S(t) = \sum_i \hbar\omega_i a_i^\dagger a_i + \sum_i \left(f_i(t)a_i^\dagger + f_i^*(t)a_i\right), \tag{15a}$$

$$H_{E\alpha} = \sum_k \hbar\omega_{\alpha k} c_{\alpha k}^\dagger c_{\alpha k}, \tag{15b}$$

$$H_{T\alpha}(t) = \hbar\sum_{ik}\left(V_{i\alpha k}(t)a_i^\dagger c_{\alpha k} + V_{i\alpha k}^*(t)c_{\alpha k}^\dagger a_i\right). \tag{15c}$$

The first part $H_S(t)$ is the Hamiltonian of the cavities in the photonic circuit and the contributions of the driving field, $f_i(t)$, acting to the cavity i (which also includes the driving field $f_{\alpha k}(t)$ acting on the waveguides in terms of the relation $f_i(t) = -V_{i\alpha k}(t)f_{\alpha k}(t)/\omega_{\alpha k}$, as shown above). The second part H_E is the Hamiltonian of the waveguides in the photonic circuit, which will be treated as reservoirs. The third part $H_T(t)$ is the coupling between the cavities and the waveguides, which can be time dependent in general through the controls of the coupling between different elements, by means of dynamically tuning the photonic structure [2,14]. With the help of the general Hamiltonian (14), various on-chip nanophotonic circuits can be modeled. For the sake of simplicity, we take $\hbar = 1$ hereafter.

3. The exact master equation for dissipative photonic dynamics

Experimentally, the photonic dynamics of resonators and the photonic transport between waveguides and resonators can be controlled by external driving fields. When a resonator exchanges particles, energy, and information with the surroundings, it becomes a typical open system. For an open quantum system, its dynamics are described by the master equation of the reduced density matrix [43]. The reduced density matrix of the resonators, denoted by $\rho(t)$, fully depicts the dynamics of photonic coherence of the driven resonators coupled with many waveguides. Any other physical observable is simply given by $\langle O(t)\rangle = \langle O\rho(t)\rangle$.

The reduced density matrix describing photonic quantum states of the driven resonators is defined by tracing over all of the waveguide degrees of freedom from the total system (the driven resonators plus the waveguides):

$$\rho(t) = \mathrm{tr}_E[\rho_{\mathrm{tot}}(t)], \tag{16}$$

where $\rho_{\mathrm{tot}}(t)$ is the density matrix of the total system. The total density matrix follows formally the evolution equation:

$$\rho_{\mathrm{tot}}(t) = U(t, t_0)\rho_{\mathrm{tot}}(t_0)U^\dagger(t, t_0), \tag{17}$$

where $U(t, t_0)$ is the evolution operator,

$$U(t, t_0) = T\exp\left\{-i\int_{t_0}^{t} H(\tau)d\tau\right\}, \tag{18}$$

in which T is the time-ordering operator, and $H(\tau)$ is the Hamiltonian of the total system given by Eq. (14). In the following, we will derive the exact master equation for the reduced density matrix by explicitly integrating out all of the waveguide degrees of freedom based on the Feynman–Vernon influence functional [26].

As usual, one can assume that there is no initial correlation between the resonators and waveguides [30], namely $\rho_{\mathrm{tot}}(t_0) = \rho(t_0)\otimes\rho_E(t_0)$, and the waveguides are initially in the equilibrium state, i.e. $\rho_E(t_0) = \frac{1}{Z}e^{-\sum_\alpha \beta_\alpha H_{E\alpha}}$, with $\beta_\alpha = 1/(k_B T_\alpha)$ and T_α is the initial temperature of the waveguide α. Then the reduced density matrix at arbitrary later time t can be expressed in the coherent state representation [44] as:

$$\langle \boldsymbol{z}_f|\rho(t)|\boldsymbol{z}_f'\rangle = \int d\mu(\boldsymbol{z}_0)d\mu(\boldsymbol{z}_0')\langle \boldsymbol{z}_0|\rho(t_0)|\boldsymbol{z}_0'\rangle \mathcal{J}(\boldsymbol{z}_f^*, \boldsymbol{z}_f', t|\boldsymbol{z}_0, \boldsymbol{z}_0'^*, t_0) \tag{19}$$

with the vector $\boldsymbol{z} = (z_1, z_2, \ldots)$ and $|\boldsymbol{z}\rangle = |z_1\rangle|z_2\rangle\cdots$ is an unnormalized multi-mode coherent state, i.e. $a_i|\boldsymbol{z}\rangle = z_i|\boldsymbol{z}\rangle$ and $\langle \boldsymbol{z}|\boldsymbol{z}'\rangle = \exp(\sum_i z_i^* z_i') = \exp(\boldsymbol{z}^\dagger\boldsymbol{z}')$, while $d\mu(\boldsymbol{z}) = \frac{d\boldsymbol{z}^* d\boldsymbol{z}}{2\pi i}e^{-|\boldsymbol{z}|^2}$ is the integral measure of the Bergman complex space [44]. The propagating function of the reduced density matrix in Eq. (19) is given in terms of the path integral:

$$\mathcal{J}(\boldsymbol{z}_f^*, \boldsymbol{z}_f', t|\boldsymbol{z}_0, \boldsymbol{z}_0'^*, t_0) = \int \mathcal{D}[\boldsymbol{z}^*\boldsymbol{z}; \boldsymbol{z}'^*\boldsymbol{z}']e^{i(S_S[\boldsymbol{z}^*,\boldsymbol{z}]-S_S^*[\boldsymbol{z}'^*,\boldsymbol{z}'])}\mathscr{F}[\boldsymbol{z}^*\boldsymbol{z}; \boldsymbol{z}'^*\boldsymbol{z}'] \tag{20}$$

with the integral boundary conditions: $\boldsymbol{z}(t_0) = \boldsymbol{z}_0$, $\boldsymbol{z}^*(t) = \boldsymbol{z}_f^*$, $\boldsymbol{z}'^*(t_0) = \boldsymbol{z}_0'^*$, and $\boldsymbol{z}'(t) = \boldsymbol{z}_f'$, where $S_S[\boldsymbol{z}^*, \boldsymbol{z}]$ is the action of the driven resonators in the coherent state representation:

$$\begin{aligned} S_S[\boldsymbol{z}^*, \boldsymbol{z}] = &-\frac{i}{2}[\boldsymbol{z}_f^\dagger\boldsymbol{z}(t) + \boldsymbol{z}^\dagger(t_0)\boldsymbol{z}_0] \\ &+ \int_{t_0}^{t} d\tau\left\{\frac{i}{2}\left[\boldsymbol{z}^\dagger\frac{d\boldsymbol{z}}{d\tau} - \frac{d\boldsymbol{z}^\dagger}{d\tau}\boldsymbol{z}\right] - (\boldsymbol{z}^\dagger\boldsymbol{\omega}\boldsymbol{z} + \boldsymbol{z}^\dagger\boldsymbol{f} + \boldsymbol{f}^\dagger\boldsymbol{z})\right\}, \end{aligned} \tag{21}$$

in which the frequency matrix $\boldsymbol{\omega} \equiv \{\omega_{ij}\}$ (here the off-diagonal matrix elements representing the possible couplings between different cavities are included for the generality of the formulation) and the driving field vector $\boldsymbol{f}(\tau) \equiv \{f_i(\tau)\}$. While $\mathscr{F}[\boldsymbol{z}^*\boldsymbol{z}; \boldsymbol{z}'^*\boldsymbol{z}']$ is the influence functional [26] obtained after integrated out all of the waveguide degrees of freedom [38,45]:

$$\begin{aligned} \mathscr{F}[\boldsymbol{z}^*\boldsymbol{z}; \boldsymbol{z}'^*\boldsymbol{z}'] = \exp\sum_\alpha\Bigg\{&-\int_{t_0}^{t} d\tau\int_{t_0}^{\tau} d\tau'\left[\boldsymbol{z}^\dagger(\tau)\mathbf{g}_\alpha(\tau, \tau')\boldsymbol{z}(\tau') + \boldsymbol{z}'^\dagger(\tau')\mathbf{g}_\alpha(\tau', \tau)\boldsymbol{z}'(\tau)\right] \\ &+ \int_{t_0}^{t} d\tau\int_{t_0}^{t} d\tau'\Big[\boldsymbol{z}'^\dagger(\tau)\mathbf{g}_\alpha(\tau, \tau')\boldsymbol{z}(\tau') \\ &- [\boldsymbol{z}^\dagger(\tau) - \boldsymbol{z}'^\dagger(\tau)]\widetilde{\mathbf{g}}_\alpha(\tau, \tau')[\boldsymbol{z}(\tau') - \boldsymbol{z}'(\tau')]\Big]\Bigg\}. \end{aligned} \tag{22}$$

The time-correlation functions in Eq. (22) are given by:

$$\mathbf{g}_{\alpha ij}(\tau,\tau') = \sum_k V_{i\alpha k}(\tau) V^*_{j\alpha k}(\tau') e^{-i\omega_{\alpha k}(\tau-\tau')}, \tag{23a}$$

$$\widetilde{\mathbf{g}}_{\alpha ij}(\tau,\tau') = \sum_k V_{i\alpha k}(\tau) V^*_{j\alpha k}(\tau') n_\alpha(\omega_{\alpha k}) e^{-i\omega_{\alpha k}(\tau-\tau')}, \tag{23b}$$

which depict the time correlations of photons in the waveguides through the resonators, and $n_\alpha(\omega_{\alpha k}) = 1/(e^{\beta_\alpha \omega_{\alpha k}} - 1)$ is the initial thermal photonic distribution function in the waveguide α at the time t_0. The influence functional, Eq. (22), contains all the back reactions from the waveguides to the driven resonators through the photonic transfer between the resonators and the waveguides. If the coupling constants do not explicitly depend on the time, then introducing the spectral density $J_\alpha(\omega) = 2\pi \sum_k V_{i\alpha k} V^*_{j\alpha k} \delta(\omega - \omega_{\alpha k})$, we can simply express the time-correlation function in terms of the spectral density as follows

$$\mathbf{g}_{\alpha ij}(\tau,\tau') = \int \frac{d\omega}{2\pi} J_\alpha(\omega) e^{-i\omega(\tau-\tau')}, \tag{24a}$$

$$\widetilde{\mathbf{g}}_{\alpha ij}(\tau,\tau') = \int \frac{d\omega}{2\pi} J_\alpha(\omega) n_\alpha(\omega) e^{-i\omega(\tau-\tau')}. \tag{24b}$$

The influence functional of Eq. (22) modifies the original action of the system into an effective one, $e^{i(S_S[\boldsymbol{z}^*,\boldsymbol{z}]-S^*_S[\boldsymbol{z}'^*,\boldsymbol{z}'])}\mathscr{F}[\boldsymbol{z}^*\boldsymbol{z};\boldsymbol{z}'^*\boldsymbol{z}'] = e^{iS_{\rm eff}[\boldsymbol{z}^*\boldsymbol{z};\boldsymbol{z}'^*\boldsymbol{z}']}$ which dramatically changes the dynamics of the driven resonators. The explicit change is manifested through the generating function of Eq. (20) by carrying out the path integral with respect to the effective action $S_{\rm eff}[\boldsymbol{z}^*\boldsymbol{z};\boldsymbol{z}'^*\boldsymbol{z}']$. While the path integral $\mathscr{D}[\boldsymbol{z}^*\boldsymbol{z};\boldsymbol{z}'^*\boldsymbol{z}']$ integrates over all the forward paths $\boldsymbol{z}^*(\tau), \boldsymbol{z}(\tau)$ and the backward paths $\boldsymbol{z}'^*(\tau), \boldsymbol{z}'(\tau)$ in the Bergman complex space bounded by $\boldsymbol{z}^*(t) = \boldsymbol{z}^*_f, \boldsymbol{z}(t_0) = \boldsymbol{z}_0$ and $\boldsymbol{z}'^*(t_0) = \boldsymbol{z}'^*_0$, $\boldsymbol{z}'(t) = \boldsymbol{z}'_f$, respectively. Since $S_{\rm eff}[\boldsymbol{z}^*\boldsymbol{z};\boldsymbol{z}'^*\boldsymbol{z}']$ is only a quadratic function in terms of the integral variables, the path integrals of Eq. (20) can be reduced to the Gaussian integrals so that we can use the stationary path method to exactly carry them out [46]. The resulting propagating function is a function of the stationary paths:

$$\begin{aligned}\mathscr{J}\left(\boldsymbol{z}^*_f, \boldsymbol{z}'_f, t | \boldsymbol{z}_0, \boldsymbol{z}'^*_0, t_0\right) = A(t) \exp\Bigg\{ &\frac{1}{2}\left[\boldsymbol{z}^\dagger_f \boldsymbol{z}(t) + \boldsymbol{z}^\dagger(t_0)\boldsymbol{z}_0 + \boldsymbol{z}'^\dagger(t)\boldsymbol{z}'_f + \boldsymbol{z}'^\dagger_0 \boldsymbol{z}'(t_0)\right] \\ &+ \frac{i}{2}\int_{t_0}^{t}\left[(\boldsymbol{z}'^\dagger(\tau) - \boldsymbol{z}^\dagger(\tau))\boldsymbol{f}(\tau) + \boldsymbol{f}^\dagger(\tau)(\boldsymbol{z}'(\tau) - \boldsymbol{z}(\tau))\right]\Bigg\},\end{aligned} \tag{25}$$

where $A(t)$ is the contribution arisen from the fluctuations around the stationary paths and is given after Eq. (31). The stationary paths obey the equations of motion:

$$\begin{aligned}&\frac{d\boldsymbol{z}(\tau)}{d\tau} + i\boldsymbol{\omega}(\tau)\boldsymbol{z}(\tau) + \int_{t_0}^{\tau} d\tau' \mathbf{g}(\tau,\tau')\boldsymbol{z}(\tau') \\ &\quad + \int_{t_0}^{t} d\tau' \widetilde{\mathbf{g}}(\tau,\tau')[\boldsymbol{z}(\tau') - \boldsymbol{z}'(\tau')] = -i\boldsymbol{f}(\tau),\end{aligned} \tag{26a}$$

$$\begin{aligned}&\frac{d\boldsymbol{z}'(\tau)}{d\tau} + i\boldsymbol{\omega}(\tau)\boldsymbol{z}'(\tau) - \int_{\tau}^{t} d\tau' \mathbf{g}(\tau,\tau')\boldsymbol{z}'(\tau') + \int_{t_0}^{t} d\tau' \mathbf{g}(\tau,\tau')\boldsymbol{z}(\tau') \\ &\quad + \int_{t_0}^{t} d\tau' \widetilde{\mathbf{g}}(\tau,\tau')[\boldsymbol{z}(\tau') - \boldsymbol{z}'(\tau')] = -i\boldsymbol{f}(\tau),\end{aligned} \tag{26b}$$

subjected to the boundary conditions $\boldsymbol{z}(t_0) = \boldsymbol{z}_0$ and $\boldsymbol{z}'(t) = \boldsymbol{z}'_f$. Here we have defined $\mathbf{g}(\tau,\tau') = \sum_\alpha \mathbf{g}_\alpha(\tau,\tau')$ and $\widetilde{\mathbf{g}}(\tau,\tau') = \sum_\alpha \widetilde{\mathbf{g}}_\alpha(\tau,\tau')$. The equations of motion for $\boldsymbol{z}^\dagger(\tau)$ and $\boldsymbol{z}'^\dagger(\tau)$ follow by exchanging $\boldsymbol{z}$ and $\boldsymbol{z}'$ in Eq. (26) and then taking conjugate transpose, subjected to the boundary conditions $\boldsymbol{z}'^\dagger(t_0) = \boldsymbol{z}'^\dagger_0$ and $\boldsymbol{z}^\dagger(t) = \boldsymbol{z}^\dagger_f$.

To express the master equation independent of the coherent state representation, we shall further factorize the boundary values of the stationary paths, $\boldsymbol{z}(t_0) = \boldsymbol{z}_0$, $\boldsymbol{z}'(t) = \boldsymbol{z}'_f$, through the following transformation:

$$\boldsymbol{z}'(\tau) - \boldsymbol{z}(\tau) = \bar{\boldsymbol{u}}(\tau, t)(\boldsymbol{z}'_f - \boldsymbol{z}(t)), \tag{27a}$$

$$\boldsymbol{z}(\tau) = \boldsymbol{u}(\tau, t_0)\boldsymbol{z}_0 + \boldsymbol{v}(\tau, t)(\boldsymbol{z}'_f - \boldsymbol{z}(t)) + \boldsymbol{y}(\tau) \tag{27b}$$

and a similar transformation for their conjugate variables (with the exchange of $\boldsymbol{z}$ with $\boldsymbol{z}'$ for the boundary values $\boldsymbol{z}^\dagger(t) = \boldsymbol{z}'^\dagger_f$ and $\boldsymbol{z}'^\dagger(t_0) = \boldsymbol{z}'^\dagger_0$), where $\boldsymbol{u}(\tau, t_0)$, $\bar{\boldsymbol{u}}(\tau, t)$, $\boldsymbol{v}(\tau, t)$ are N by N matrices, and $\boldsymbol{y}(\tau)$ is $1 \times N$ matrix, N is the dimension of the cavity system. From Eq. (26), we find that these functions obey the equations of motion

$$\frac{d\boldsymbol{u}(\tau, t_0)}{d\tau} + i\boldsymbol{\omega}\boldsymbol{u}(\tau, t_0) + \int_{t_0}^{\tau} \mathbf{g}(\tau, \tau')\boldsymbol{u}(\tau', t_0)d\tau' = 0, \tag{28a}$$

$$\frac{d\bar{\boldsymbol{u}}(\tau, t)}{d\tau} + i\boldsymbol{\omega}\bar{\boldsymbol{u}}(\tau, t) - \int_{\tau}^{t} \mathbf{g}(\tau, \tau')\bar{\boldsymbol{u}}(\tau', t)d\tau' = 0, \tag{28b}$$

$$\frac{d\boldsymbol{v}(\tau, t)}{d\tau} + i\boldsymbol{\omega}\boldsymbol{v}(\tau, t) + \int_{t_0}^{\tau} \mathbf{g}(\tau, \tau')\boldsymbol{v}(\tau', t)d\tau' = \int_{t_0}^{t} \widetilde{\mathbf{g}}(\tau, \tau')\bar{\boldsymbol{u}}(\tau', t)d\tau', \tag{28c}$$

$$\frac{d\boldsymbol{y}(\tau)}{d\tau} + i\boldsymbol{\omega}\boldsymbol{y}(\tau) + \int_{t_0}^{\tau} \mathbf{g}(\tau, \tau')\boldsymbol{y}(\tau')d\tau' = -i\boldsymbol{f}(\tau) \tag{28d}$$

subjected to the conditions $\bar{\boldsymbol{u}}(t, t) = 1$, $\boldsymbol{u}(t_0, t_0) = 1$, $\boldsymbol{v}(t_0, t) = 0$ and $\boldsymbol{y}(t_0) = 0$ with $t_0 \le \tau, \tau' \le t$. It is not too difficult to find that

$$\bar{\boldsymbol{u}}(\tau, t) = \boldsymbol{u}^\dagger(t, \tau), \tag{29a}$$

$$\boldsymbol{y}(\tau) = -i\int_{t_0}^{\tau} \boldsymbol{u}(\tau, \tau')\boldsymbol{f}(\tau')d\tau', \tag{29b}$$

$$\boldsymbol{v}(\tau, t) = \int_{t_0}^{\tau} d\tau' \int_{t_0}^{t} d\tau'' \boldsymbol{u}(\tau, \tau')\widetilde{\mathbf{g}}(\tau', \tau'')\bar{\boldsymbol{u}}(\tau'', t). \tag{29c}$$

Now, let $\tau = t_0$ in Eq. (27a) and $\tau = t$ in Eq. (27b), $\boldsymbol{z}(t)$ and $\boldsymbol{z}'(t_0)$ can be expressed in terms of the boundary conditions $\boldsymbol{z}_0$ and $\boldsymbol{z}'_f$:

$$\boldsymbol{z}(t) = \boldsymbol{w}(t)\big[\boldsymbol{u}(t, t_0)\boldsymbol{z}_0 + \boldsymbol{v}(t, t)\boldsymbol{z}'_f + \boldsymbol{y}(t)\big], \tag{30a}$$

$$\begin{aligned}\boldsymbol{z}'(t_0) \;=\; & \boldsymbol{u}^\dagger(t, t_0)\left[1 - \boldsymbol{w}(t)\boldsymbol{v}(t, t)\right]\boldsymbol{z}'_f - \boldsymbol{u}^\dagger(t, t_0)\boldsymbol{w}(t)\boldsymbol{y}(t) \\ & + \left[1 - \boldsymbol{u}^\dagger(t, t_0)\boldsymbol{w}(t)\boldsymbol{u}(t, t_0)\right]\boldsymbol{z}_0,\end{aligned} \tag{30b}$$

here $\boldsymbol{w}(t) = [\mathbf{1} + \boldsymbol{v}(t, t)]^{-1} = \boldsymbol{w}^\dagger(t)$. Similarly, $\boldsymbol{z}^\dagger(t_0)$ and $\boldsymbol{z}'^\dagger(t)$ can be obtained by exchanging $\boldsymbol{z}$ and $\boldsymbol{z}'$ in Eq. (30) and taking a conjugate transpose. Substituting these results with Eq. (27) into Eq. (25), we obtain the final form of the propagating function for the reduced density matrix

$$\begin{aligned}\mathcal{J}\left(\boldsymbol{z}^*_f, \boldsymbol{z}'_f, t|\boldsymbol{z}_0, \boldsymbol{z}'^*_0, t_0\right) = A(t)\exp\Big\{ & (\boldsymbol{z}^\dagger_f - \boldsymbol{y}^\dagger(t))\boldsymbol{J}_1(t)\boldsymbol{z}_0 + \boldsymbol{z}'^\dagger_0\boldsymbol{J}^\dagger_1(t)(\boldsymbol{z}'_f - \boldsymbol{y}(t)) \\ & + \boldsymbol{z}^\dagger_f\boldsymbol{J}_2(t)\boldsymbol{z}'_f + \boldsymbol{z}'^\dagger_0\boldsymbol{J}_3(t)\boldsymbol{z}_0 - \boldsymbol{z}^\dagger_f\boldsymbol{y}(t) - \boldsymbol{y}^\dagger(t)\boldsymbol{z}'_f - \boldsymbol{y}^\dagger(t)\boldsymbol{w}(t)\boldsymbol{y}(t)\Big\},\end{aligned} \tag{31}$$

in which $A(t) = \det[\boldsymbol{w}(t)]$, $\boldsymbol{J}_1(t) = \boldsymbol{w}(t)\boldsymbol{u}(t, t_0)$, $\boldsymbol{J}_2(t) = 1 - \boldsymbol{w}(t)$, $\boldsymbol{J}_3(t) = 1 - \boldsymbol{u}^\dagger(t, t_0)\boldsymbol{w}(t)\boldsymbol{u}(t, t_0)$ and $\boldsymbol{w}(t) = [\mathbf{1} + \boldsymbol{v}(t, t)]^{-1} = \boldsymbol{w}^\dagger(t)$.

Substituting Eq. (31) into Eq. (19), taking a time derivative to the reduced density matrix, and then using the relations [44]: $a_i|\boldsymbol{z}\rangle = z_i|\boldsymbol{z}\rangle$ and $\frac{\partial}{\partial z_i}|\boldsymbol{z}\rangle = a_i^\dagger|\boldsymbol{z}\rangle$, a time convolutionless but exact master equation is obtained for the driving resonator system coupled to the waveguides:

$$\begin{aligned}\frac{d\rho(t)}{dt} &= -i\,[H_{\rm eff}(t),\,\rho(t)] + \sum_{ij}\gamma_{ij}(t)\left[2a_j\rho(t)a_i^\dagger - \rho(t)a_i^\dagger a_j - a_i^\dagger a_j\rho(t)\right]\\ &\quad + \sum_{ij}\widetilde{\gamma}_{ij}(t)\left[a_j\rho(t)a_i^\dagger + a_i^\dagger\rho(t)a_j - a_i^\dagger a_j\rho(t) - \rho(t)a_j a_i^\dagger\right]\\ &= -i[H_{\rm eff}(t),\,\rho(t)] + \sum_{ij}(2\gamma_{ij}(t) + \widetilde{\gamma}_{ij}(t))\left[a_j\rho(t)a_i^\dagger - \frac{1}{2}(a_i^\dagger a_j\rho(t) + \rho(t)a_i^\dagger a_j)\right]\\ &\quad + \sum_{ij}\widetilde{\gamma}_{ij}(t)\Big[a_i^\dagger\rho(t)a_j - \frac{1}{2}(a_j a_i^\dagger\rho(t) + \rho(t)a_j a_i^\dagger)\Big],\end{aligned} \tag{32}$$

where $H_{\rm eff}(t) = \sum_{ij}\omega'_{ij}(t)a_i^\dagger a_j + \sum_i[f'_i(t)a_i^\dagger + f'^*_i(t)a_i]$ is the effective Hamiltonian of the driven resonators. The renormalized frequencies $\omega'_{ij}(t)$ and the renormalized driving field $f'_i(t)$ are results of the back-reaction of the waveguides. The initial temperature effects are fully incorporated into the temperature-dependent noise coefficient $\widetilde{\boldsymbol{\gamma}}(t)$. The time dependent dissipation coefficients $\boldsymbol{\gamma}$(t) together with the time-dependent noise coefficients $\widetilde{\boldsymbol{\gamma}}(t)$ describe the non-Markovian dissipation and decoherence dynamics of the resonators due to the interaction between the resonators and waveguides. These coefficients also describe the photonic transport in the system, as we will show in the next section. All these time-dependent coefficients are given explicitly

$$\omega'_{ij}(t) = \frac{i}{2}\left[\frac{d\boldsymbol{u}(t,t_0)}{dt}\boldsymbol{u}^{-1}(t,t_0) - \text{H.c.}\right]_{ij}, \tag{33a}$$

$$\gamma_{ij}(t) = -\frac{1}{2}\left[\frac{d\boldsymbol{u}(t,t_0)}{dt}\boldsymbol{u}^{-1}(t,t_0) + \text{H.c.}\right]_{ij}, \tag{33b}$$

$$\widetilde{\gamma}_{ij}(t) = \frac{d\boldsymbol{v}_{ij}(t,t)}{dt} - \left[\frac{d\boldsymbol{u}(t,t_0)}{dt}\boldsymbol{u}^{-1}(t,t_0)\boldsymbol{v}(t,t) + \text{H.c.}\right]_{ij}, \tag{33c}$$

$$f'_i(t) = i\frac{d\boldsymbol{y}_i(t)}{dt} - i\left[\frac{d\boldsymbol{u}(t,t_0)}{dt}\boldsymbol{u}^{-1}(t,t_0)\boldsymbol{y}(t)\right]_i, \tag{33d}$$

as functions of $\boldsymbol{u}(t,t_0)$, $\boldsymbol{v}(t,t)$ and $\boldsymbol{y}(t)$ that are determined by the integrodifferential equations of Eq. (28). We should point out that although the master equation of Eq. (32) has a time convolutionless form, it is exact. The non-Markovian memory effect between the resonators and the waveguides is fully embodied non-perturbatively in the integral kernels of Eq. (28). These integral kernels contain the non-local time-correlation functions of the waveguides, $\mathbf{g}(\tau,\tau')$ and $\widetilde{\mathbf{g}}(\tau,\tau')$, that describe the non-Markovian memory processes.

Besides, in the second equality of (32) we have rewritten the master equation in terms of the standard Lindblad–Gorini–Kossakowski–Sudarshan (LGKS) form [47,48]. However, different from the original LGKS form [47,48], the master equation obtained here is exact and is derived at the microscopic level. The dissipation and fluctuation coefficients, $\boldsymbol{\gamma}$(t) and $\widetilde{\boldsymbol{\gamma}}(t)$ in the master equation, are time-dependent and are determined nonperturbatively and exactly by the functions $\boldsymbol{u}(t,t_0)$, $\boldsymbol{v}(t,t)$. The functions $\boldsymbol{u}(t,t_0)$, $\boldsymbol{v}(t,t)$ are indeed Keldysh's nonequilibrium Green functions [24], as we will show in the next section. Notice that using the Feynman–Vernon influence functional approach to derive the exact master equation was previously carried out only for quantum Brown motion (QBM) [33,49]. The exact master equation of QBM can also be obtained by the trace-over-bath on total-space Wigner-function method [50] or the stochastic diffusion Schrödinger equation [51]. All these previous works deal mainly with a single harmonic oscillator coupled to a thermal bath without external driving fields. The extension of the exact master equation to the systems of two entangled

optical modes or two entangled harmonic oscillators has been worked out very recently [45,52,53]. The extension of the exact quantum master equation for a driven Brownian oscillator is also recently given via a Wigner phase-space Gaussian wave packet approach [54]. Here the exact master equation of Eq. (32) is the most general one for the system containing arbitrary number of entangled modes coupled to arbitrary number of photonic reservoirs with arbitrary spectral density at arbitrary initial temperatures and applied with arbitrary number of external driving fields. It allows to investigate various exact non-Markovian dynamics in photonic systems.

In fact, the master equation (32) determines all the nonequilibrium dynamics of the driven resonators and the photonic transport between the resonators and the waveguides in nanophotonics. The aim of the present paper is to use the exact master equation derived above to establish a quantum dissipative transport theory that generalizes the quantum transport theory based on Keldysh's nonequilibrium Green function technique. We will show in the next section how the photocurrents passing through the resonators into waveguides can be obtained directly from the master equation, and how the quantum transport theory based on Keldysh's nonequilibrium Green function technique can be easily reproduced and generalized.

4. Photonic transport in nanophotonic circuits

In this section, the exact photocurrent in photonic circuits is derived. The connection between the photocurrent and the master equation of the reduced density matrix is given, which explicitly demonstrates the intimacy between quantum coherence and quantum transport in nonequilibrium dynamics. The relation between the transport theory obtained here and the transport theory based on Keldysh's nonequilibrium Green function technique is also presented, and the power of the present theory is discussed.

4.1. The time evolution of the cavity field and intensity

Before we derive the photocurrent, we shall compute from the exact master equation two important physical observables describing the photonic dynamics of the driven resonators. One of them is the time evolution of the photonic resonator field, another one is the single particle reduced density matrix which characterizes photonic intensity of the resonators.

The photonic field of the resonators is determined by $\langle a_i(t)\rangle = \mathrm{tr}_s[a_i\rho(t)]$. With the help of Eq. (32), it obeys the equation of motion:

$$\frac{d}{dt}\langle a_i(t)\rangle = \sum_j \left[\frac{d\boldsymbol{u}(t,t_0)}{dt}\boldsymbol{u}^{-1}(t,t_0)\right]_{ij}\langle a_j(t)\rangle - if_i'(t). \tag{34}$$

Its solution is:

$$\langle a_i(t)\rangle = \sum_j u_{ij}(t,t_0)\langle a_j(t_0)\rangle + y_i(t). \tag{35}$$

In other words, the photonic field of the driven resonators is a combination of the photonic propagating of the initial field $\boldsymbol{u}(t,t_0)\langle a_j(t_0)\rangle$ and the driving-induced field $\boldsymbol{y}(t)$ (see Eq. (29b)). This solution describes the driving-field-induced photonic coherence in the resonators. Similarly, the equation of motion for the single particle reduced density matrix of the resonators, $\rho_{ij}^{(1)}(t) = \mathrm{tr}_s[a_j^\dagger a_i\rho(t)]$, can also be found from the exact master equation:

$$\begin{aligned}\frac{d}{dt}\rho_{ij}^{(1)}(t) &= i\langle a_i(t)\rangle f_j'^{\dagger}(t) - if_i'(t)\langle a_j^\dagger(t)\rangle + \widetilde{\gamma}_{ij}(t)\\ &\quad + \sum_m \left\{\left[\frac{d\boldsymbol{u}(t,t_0)}{dt}\boldsymbol{u}^{-1}(t,t_0)\right]_{im}\rho_{mj}^{(1)}(t) + \rho_{im}^{(1)}(t)\left[\frac{d\boldsymbol{u}(t,t_0)}{dt}\boldsymbol{u}^{-1}(t,t_0)\right]_{mj}^{\dagger}\right\}.\end{aligned} \tag{36}$$

The solution of the above equation of motion can be expressed explicitly in terms of the functions $\boldsymbol{u}(t,t_0)$, $\boldsymbol{v}(t,t)$ and the driving-induced field $\boldsymbol{y}(t)$:

$$\rho_{ij}^{(1)}(t) = \langle a_i(t)\rangle y_j^*(t) + y_i(t)\langle a_j^\dagger(t)\rangle - y_i(t)y_j^*(t) + v_{ij}(t,t) + \sum_{mn} u_{im}(t,t_0)\rho_{mn}^{(1)}(t_0)u_{ni}^*(t,t_0). \tag{37}$$

The first three terms in the above solution are the contribution coming from the driving fields. The fourth term is the contribution from the thermal fluctuation of the waveguides (see the solution of $\boldsymbol{v}(t,t)$ by Eq. (29c)), and the last term comes from the initial photonic distribution in the resonators. Besides, the i-th diagonal element of the single particle reduced density matrix gives the average photon number of the mode i in the resonators, i.e.

$$\rho_{ii}^{(1)}(t) = \mathrm{tr}_s[a_i^\dagger a_i \rho(t)] = n_i(t), \tag{38}$$

which measures the photonic intensity of the resonators. The photonic coherence and the photonic intensity of the driven resonators, given respectively by Eqs. (35) and (38), play an important role for photonic transport, as we shall discuss in the next.

4.2. Photocurrent in each waveguide channel

To find the photocurrent flowing from the resonators to each waveguide, it will be more convenient to reexpress the master equation, Eq. (32), as follows:

$$\frac{d\rho(t)}{dt} = -i[H_S(t),\rho(t)] + \sum_\alpha \left[\mathcal{L}_\alpha^+(t) + \mathcal{L}_\alpha^-(t)\right]\rho(t) - i\sum_\alpha \left[f_{\alpha i}(t)a_i^\dagger + f_{\alpha i}^*(t)a_i, \rho(t)\right]. \tag{39}$$

Here $H_S(t)$ is the original Hamiltonian of Eq. (15a) for the driven resonators. $\mathcal{L}_\alpha^+(t)$ and $\mathcal{L}_\alpha^-(t)$ are superoperators acting on the reduced density matrix, induced by the coupling to the waveguides. They are given by:

$$\mathcal{L}_\alpha^+(t)\rho(t) = \sum_{ij}\left\{\lambda_{\alpha ij}(t)[a_j\rho(t)a_i^\dagger - \rho(t)a_j a_i^\dagger] - \kappa_{\alpha ij}(t)a_i^\dagger a_j\rho(t) + \mathrm{H.c.}\right\}, \tag{40a}$$

$$\mathcal{L}_\alpha^-(t)\rho(t) = \sum_{ij}\left\{\lambda_{\alpha ij}(t)[a_i^\dagger\rho(t)a_j - a_i^\dagger a_j\rho(t)] + \kappa_{\alpha ij}(t)a_j\rho(t)a_i^\dagger + \mathrm{H.c.}\right\} \tag{40b}$$

with the coefficients

$$\boldsymbol{\kappa}_\alpha(t) = \int_{t_0}^t d\tau \mathbf{g}_\alpha(t,\tau)\boldsymbol{u}(\tau,t_0)\boldsymbol{u}^{-1}(t,t_0), \tag{41a}$$

$$\boldsymbol{\lambda}_\alpha(t) = \int_{t_0}^t d\tau\,[\mathbf{g}_\alpha(t,\tau)\boldsymbol{v}(\tau,t) - \widetilde{\mathbf{g}}_\alpha(t,\tau)\bar{\boldsymbol{u}}(\tau,t)] - \boldsymbol{\kappa}_\alpha(t)\boldsymbol{v}(t,t). \tag{41b}$$

These time coefficients are related with the time-dependent dissipation and fluctuation coefficients in the master equation of Eq. (32) by

$$\omega'_{ij}(t) = \omega_{ij}(t) - \frac{i}{2}\sum_\alpha\left[\boldsymbol{\kappa}_\alpha(t) - \boldsymbol{\kappa}_\alpha^\dagger(t)\right]_{ij}, \tag{42a}$$

$$\gamma_{ij}(t) = \frac{1}{2}\sum_\alpha\left[\boldsymbol{\kappa}_\alpha(t) + \boldsymbol{\kappa}_\alpha^\dagger(t)\right]_{ij}, \qquad \widetilde{\gamma}_{ij}(t) = \sum_\alpha[\boldsymbol{\lambda}_\alpha(t) + \boldsymbol{\lambda}_\alpha^\dagger(t)]_{ij}. \tag{42b}$$

The superoperators $\mathcal{L}_\alpha^+(t)$ and $\mathcal{L}_\alpha^-(t)$ are intimately related to the photocurrent through the waveguide α, as we will see next. The last term in Eq. (39) is the reservoir-induced effective driving fields:

$$\boldsymbol{f}_\alpha(t) = i\boldsymbol{\kappa}_\alpha(t)\boldsymbol{y}(t) - i\int_{t_0}^{t} d\tau \mathbf{g}_\alpha(t,\tau)\boldsymbol{y}(\tau) \tag{43}$$

which shifts the driving fields $\boldsymbol{f}(t)$ to the renormalized fields $f_i'(t) = f_i(t) + \sum_\alpha [\boldsymbol{f}_\alpha(t)]_i$ in Eq. (32). In other words, $\boldsymbol{f}_\alpha(t)$ is a feed-back effect of the system–reservoir coupling to the external driving field.

The photocurrent flowing from the resonators into the waveguide α is defined in the Heisenberg picture as:

$$\begin{aligned} I_\alpha(t) &\equiv \frac{d\langle N_\alpha(t)\rangle}{dt} = -i\langle [N_\alpha(t), H(t)]\rangle \\ &= i\sum_{ki}\left[V_{i\alpha k}(t)\left\langle a_i^\dagger(t)c_{\alpha k}(t)\right\rangle - V_{i\alpha k}^*(t)\left\langle a_i^\dagger(t)c_{\alpha k}(t)\right\rangle\right], \end{aligned} \tag{44}$$

where $N_\alpha = \sum_k c_{\alpha k}^\dagger c_{\alpha k}$ is the photon number operator of the waveguide α. Furthermore, consider the single particle reduced density matrix in the Heisenberg picture: $\rho_{ij}^{(1)}(t) = \mathrm{tr}_s[a_j^\dagger a_i \rho(t)] = \langle a_j^\dagger(t) a_i(t)\rangle$, we find that

$$\frac{d\boldsymbol{\rho}^{(1)}(t)}{dt} = -i[\boldsymbol{\omega}, \boldsymbol{\rho}^{(1)}(t)] + \mathcal{S}(t) - \sum_\alpha \mathcal{I}_\alpha(t), \tag{45}$$

where $\mathcal{I}_\alpha(t)$ and $\mathcal{S}(t)$ are the current matrix of the waveguide α and the source matrix of the driven resonators:

$$\mathcal{S}_{ij}(t) = i\langle a_i(t)\rangle f_j^*(t) - i f_i(t)\langle a_j^\dagger(t)\rangle, \tag{46a}$$

$$\mathcal{I}_{\alpha ij}(t) = i\sum_k \left[V_{i\alpha k}(t)\langle a_j^\dagger(t)c_{\alpha k}(t)\rangle - V_{j\alpha k}^*(t)\langle a_i^\dagger(t)c_{\alpha k}\rangle\right]. \tag{46b}$$

Comparing Eqs. (44) and (46b), one can see that the trace of the current matrix is just the photocurrent flowing from the resonators into the waveguide α: $I_\alpha(t) = \mathrm{Tr}[\mathcal{I}_\alpha(t)]$. Note that Tr is the trace over the $N \times N$ matrix of the N single modes in the resonators, while tr_s and tr_E used before denote the traces over all the quantum states of the resonators and the waveguides, respectively.

On the other hand, the equation of motion for the single particle reduced density matrix can also be obtained directly from the master equation, Eq. (39). The result is

$$\frac{d}{dt}\rho_{ij}^{(1)}(t) = -i[\boldsymbol{\omega}, \boldsymbol{\rho}^{(1)}(t)]_{ij} + S_{ij}(t) + \sum_\alpha \mathrm{tr}_s\left[a_j^\dagger a_i\left[\mathcal{L}_\alpha^+(t) + \mathcal{L}_\alpha^-(t)\right]\rho(t)\right]. \tag{47}$$

Comparing Eqs. (45) and (47) for the single particle reduced density matrix, with the help of Eqs. (40) and (41), we obtain the explicit formula for the photocurrent matrix:

$$\mathcal{I}_\alpha(t) = \int_{t_0}^{t} d\tau \left\{\mathbf{g}_\alpha(t,\tau)\boldsymbol{\rho}^{(1)}(\tau,t) - \widetilde{\mathbf{g}}_\alpha(t,\tau)\bar{\boldsymbol{u}}(\tau,t) + \mathrm{H.c.}\right\} \tag{48}$$

and $\boldsymbol{\rho}^{(1)}(\tau,t)$ is the generalized correlation function which is given explicitly by:

$$\begin{aligned} \rho_{ij}^{(1)}(\tau,t) &= \sum_{mn} u_{im}(\tau,t_0)\rho_{mn}^{(1)}(t_0)u_{ni}^*(t,t_0) + v_{ij}(\tau,t) + y_i(\tau)y_j^*(t) \\ &\quad + \sum_m [u_{im}(\tau,t_0)\langle a_m(t_0)\rangle y_j^*(t) + y_i(\tau)\langle a_m^\dagger(t_0)\rangle u_{mj}^*(t,t_0)]. \end{aligned} \tag{49}$$

Then the photocurrent flowing into the waveguide α is simply given by:

$$\begin{aligned} I_\alpha(t) &= \mathrm{tr}_s[\mathcal{L}_\alpha^+(t)\rho(t)] = -\mathrm{tr}_s[\mathcal{L}_\alpha^-(t)\rho(t)] \\ &= 2\mathrm{Re}\int_{t_0}^{t} d\tau \mathrm{Tr}[\mathbf{g}_\alpha(t,\tau)\boldsymbol{\rho}^{(1)}(\tau,t) - \widetilde{\mathbf{g}}_\alpha(t,\tau)\bar{\boldsymbol{u}}(\tau,t)]. \end{aligned} \tag{50}$$

It shows that the photocurrent is completely determined by the time-correlation functions $\mathbf{g}_\alpha(t,\tau)$ and $\widetilde{\mathbf{g}}_\alpha(t,\tau)$ of the waveguides and the propagating and correlation functions $\bar{\boldsymbol{u}}(\tau,t)$ and $\boldsymbol{\rho}^{(1)}(\tau,t)$ of the driven resonators. The time-correlation functions of the waveguides characterize the non-Markovian memory structure of the photon transfer between resonators and waveguides, while the propagating and correlation functions depict the photon coherence and photon correlation of the resonators under the control of the external driving fields.

In fact, Eq. (45) is a generalized quantum continuous equation. By tracing over the equation of motion for the single particle reduced density matrix, we have

$$\frac{dN}{dt} = S(t) - \sum_\alpha I_\alpha(t). \tag{51}$$

Here $N(t) = \mathrm{Tr}[\boldsymbol{\rho}^{(1)}(t)]$ is the total photon number in the resonators, $S(t) = \mathrm{Tr}[\mathcal{S}(t)]$ is the source coming from the driving fields, and $I_\alpha(t) = \mathrm{Tr}[\mathcal{I}_\alpha(t)]$ is the photocurrent flowing into the waveguides α. Eq. (51) tells that the increase of the photon number in the resonators equals to the photons received from the driving field subtract the photons flow into the waveguides.

4.3. Relations to Keldysh's nonequilibrium Green functions

As one seen from Eq. (50), the photocurrent is completely determined by the time-correlation functions $\mathbf{g}_\alpha(t,\tau)$ and $\widetilde{\mathbf{g}}_\alpha(t,\tau)$ of the waveguides plus the propagating and correlation functions $\bar{\boldsymbol{u}}(\tau,t)$ and $\boldsymbol{\rho}^{(1)}(\tau,t)$ of the driven resonators. In fact, it has been shown [39] that the functions $\boldsymbol{u}(\tau,t_0)$, $\bar{\boldsymbol{u}}(\tau,t)$, $\boldsymbol{\rho}^{(1)}(\tau,t)$ are the retarded, advanced and lesser Green functions of the resonators in Keldysh's nonequilibrium formalism [24,25,27,29]:

$$u_{ij}(t_1,t_2) = \theta(t_1-t_2)\left\langle\left[a_i(t_1), a_j^\dagger(t_2)\right]\right\rangle \equiv iG^r_{ij}(t_1,t_2), \tag{52a}$$

$$\bar{u}_{ij}(t_1,t_2) = \theta(t_2-t_1)\left\langle\left[a_i(t_1), a_j^\dagger(t_2)\right]\right\rangle \equiv -iG^a_{ij}(t_1,t_2), \tag{52b}$$

$$\rho^{(1)}_{ij}(t_1,t_2) = \left\langle a_j^\dagger(t_2)a_i(t_1)\right\rangle \equiv -iG^<_{ij}(t_1,t_2). \tag{52c}$$

While, the time-correlation functions $\mathbf{g}_\alpha(t,\tau)$ and $\widetilde{\mathbf{g}}_\alpha(t,\tau)$ correspond to the retarded and lesser self-energy functions arose from the couplings between the resonators and the waveguides:

$$\mathbf{g}_{\alpha ij}(t_1,t_2) = i\sum_{\alpha ij}^{r}(t_1,t_2), \qquad \widetilde{\mathbf{g}}_{\alpha ij}(t_1,t_2) = -i\sum_{\alpha ij}^{<}(t_1,t_2). \tag{53a}$$

The explicit form of these self-energy functions is given by Eq. (23) or (24) which is rather simple. In Keldysh's nonequilibrium Green function technique, quantum transport theory is completely expressed in terms of the retarded, advanced and lesser Green functions.

Explicitly, Eq. (28a) for $\boldsymbol{u}(\tau,t_0)$ obtained in the last section can be rewritten as:

$$\left\{i\frac{d}{d\tau} - \boldsymbol{\omega}\right\}\boldsymbol{G}^r(\tau,t_0) = \delta(\tau-t_0) + \int_{t_0}^{\tau}\boldsymbol{\Sigma}^r(\tau,\tau')\boldsymbol{G}^r(\tau',t_0)d\tau' \tag{54}$$

which is just the standard Dyson equation for the retarded Green function. The advanced Green function obeys the relation: $\boldsymbol{G}^a(t_1,t_2) = [\boldsymbol{G}^r(t_2,t_1)]^\dagger$, see Eq. (29a). The crucial and also the most difficult part in Keldysh's nonequilibrium Green function technique is the calculation of the lesser Green function $\boldsymbol{G}^<(\tau,t)$. The lesser Green function $\boldsymbol{G}^<(t_1,t_2)$ fully determines the quantum kinetics of nonequilibrium systems. From Eq. (49), the exact analytical solution of the lesser Green function is already given:

$$\begin{aligned}\boldsymbol{G}^<(\tau,t) =\ & i\boldsymbol{y}(\tau)\boldsymbol{y}^\dagger(t) - \boldsymbol{G}^r(\tau,t_0)\langle\boldsymbol{a}^\dagger(t_0)\rangle\boldsymbol{y}^\dagger(t) + \boldsymbol{y}(\tau)\langle\boldsymbol{a}(t_0)\rangle\boldsymbol{G}^a(t_0,t)\\ &+ \boldsymbol{G}^r(\tau,t_0)\boldsymbol{G}^<(t_0,t_0)\boldsymbol{G}^a(t_0,t)\\ &+ \int_{t_0}^{\tau}d\tau_1\int_{t_0}^{t}d\tau_2\,\boldsymbol{G}^r(\tau,\tau_1)\boldsymbol{\Sigma}^<(\tau_1,\tau_2)\boldsymbol{G}^a(\tau_2,t),\end{aligned} \tag{55}$$

where $\boldsymbol{G}^<(t_0, t_0) = i\boldsymbol{\rho}^{(1)}(t_0)$ is the initial photon distribution in the resonators, $\langle \boldsymbol{a}(t_0)\rangle$ is the initial resonator fields, and $\boldsymbol{y}(t)$ is the driving-induced resonator field given by Eq. (29b).

Comparing with the electron transport in mesoscopic systems, one always has $\langle \boldsymbol{a}^\dagger(t_0)\rangle = \langle \boldsymbol{a}(t_0)\rangle = 0$ for electrons. Also, one usually ignores the first term in the standard Green function calculation by taking $t_0 \to -\infty$ which loses the information of the initial state dependence in quantum transport, an important effect for non-Markovian memory dynamics. Besides, the external driving fields applied to the leads and gates in mesoscopic systems are embedded into the spectral densities or the energy levels in the central region so that no extra driving-induced field is produced, namely $\boldsymbol{y}(t) = 0$. Thus, the resulting lesser Green function obtained in the mesoscopic electron transport contains only the last term in Eq. (55) [29]. In other words, Eq. (55) gives the exact and general solution for the lesser Green function for photonic systems. With the above relations and solutions, the photocurrent, Eq. (50), can be re-expressed as:

$$I_\alpha(t) = 2\mathrm{Re}\int_{t_0}^{t} d\tau \mathrm{Tr}[\boldsymbol{\Sigma}_\alpha^r(t,\tau)\boldsymbol{G}^<(\tau,t) + \boldsymbol{\Sigma}_\alpha^<(t,\tau)\boldsymbol{G}^a(\tau,t)]. \tag{56}$$

This reproduces the standard transport current in Keldysh's nonequilibrium Green function technique that has been widely used in the investigation of various electron transport phenomena in mesoscopic systems, although most of the previous works used only the special solution of the lesser Green function, as we just discussed above.

In conclusion, a full quantum transport theory for photonic circuitry has been established from the Feynman–Vernon influence functional approach. In the literature, the investigation of quantum transport mainly uses Keldysh's nonequilibrium Green function technique. Keldysh's nonequilibrium Green function technique has the advantage of treating the lesser Green function in a complicated system by the assumption of adiabatically switching on the many-body correlations. This allows one to trace back the initial time $t_0 \to -\infty$, which provides a great simplification for practical evaluation but meantime it lacks a proper treatment for transient phenomena. The Feynman–Vernon influence functional aims to address dissipative dynamics of an open system in terms of the reduced density matrix. The master equation derived from the influence functional explicitly determines, by definition, the temporal evolution of an initially prepared state. For nanophotonic devices, when the many-photon correlations become less important and can be ignored, we are able to obtain the exact master equation where all the non-Markovian memory effects are encoded into the time-dependent coefficients in the master equation. It turns out that these time-dependent coefficients are determined indeed by the retarded and lesser Green functions in Keldysh's formalism, as we have just shown. Therefore, all the advantages of the nonequilibrium Green function technique are maintained in our theory but the difficulty in addressing the transient dynamics in the Green function technique is avoided in terms of the master equation. As a result, two fundamental nonequilibrium approaches, the Schwinger–Keldysh nonequilibrium Green function technique and the Feynman–Vernon influence functional approach, is unified, which makes the transport theory very powerful in the study of the transient transport phenomena in nonequilibrium photonic systems.

5. Analytical and numerical illustration

5.1. Modeling a nanophotonic transistor

In this section, the theory developed in the previous sections is applied to a specific photonic circuit in photonic crystals, a nanophotonic transistor, as an illustration. A physical realization of the on-chip nanophotonic circuit described in Section 2 is a device of one or a few nanocavities coupled to many waveguides in the photonic crystals, as schematically shown by Fig. 1. Here the nanocavity can be considered as a point defect created in photonic crystals as a resonator [3]. Its frequency can be easily tuned to any value within the band gap by changing the size or the shape of the defect. While, a waveguide in photonic crystals can also be considered as a series of coupled point defects in which photon propagates due to the coupling of the adjacent defects [4,5]. By changing the modes of the resonators and the coupling configuration through various techniques [10–13], the

transmission properties of the waveguide can also be manipulated. In principle, one can solve Eq. (6) to obtain the dispersion relations of the waveguides and the couplings between the cavities and waveguides [1,9]. Here we may treat the waveguide as a tight-binding model, namely the Hamiltonian of the waveguide and the coupling Hamiltonian between the nanocavities and the waveguide can be expressed explicitly as [23]:

$$H_{E\alpha} = \sum_n \omega_\alpha c^\dagger_{\alpha n} c_{\alpha n} - \sum_{n=1} \xi_\alpha (c^\dagger_{\alpha n} c_{\alpha n+1} + \text{H.c.}), \tag{57a}$$

$$H_{T\alpha} = \xi_{i\alpha n_i} (a^\dagger_i c_{\alpha n_i} + \text{H.c.}) \tag{57b}$$

where ξ_α is the hopping rate between adjacent resonator modes within the waveguide α, and it is experimentally turnable. $\xi_{i\alpha n_i}$ is the coupling constant of the ith nanocavity coupled to the nth resonator in the waveguide α, which is also controllable by changing the geometrical parameters of the defect cavity and the distance between the cavities and the waveguide [55].

Furthermore, making the Fourier transform for semi-infinite waveguide,

$$c_{\alpha k} = \sqrt{\frac{2}{\pi}} \sum_{n=1}^{\infty} \sin(nk) c_{\alpha n}, \tag{58}$$

we can transform the Hamiltonian of Eq. (57) from the spatial space into the wavevector space with the result:

$$H_{E\alpha} = \sum_k \omega_{\alpha k} c^\dagger_{\alpha k} c_{\alpha k}, \tag{59a}$$

$$H_{T\alpha} = \sum_k \left(V_{i\alpha k} a^\dagger_i c_{\alpha k} + \text{H.c.} \right), \tag{59b}$$

where $0 \le k \le \pi$, and $\omega_{\alpha k}$ and $V_{i\alpha k}$ are given by:

$$\omega_{\alpha k} = \omega_\alpha - 2\xi_\alpha \cos(k), \qquad V_{i\alpha k} = \sqrt{\frac{2}{\pi}}\, \xi_{i\alpha n_i} \sin(n_i k), \tag{60}$$

and $c^\dagger_{\alpha k}$, $c_{\alpha k}$ are the creation and annihilation operators of the corresponding Bloch modes in the waveguide α.

More specifically, for the photonic circuit consisting of N nanocavities coupled to one waveguide at different sites $\{n_i\}$, the total Hamiltonian of the system can be rewritten explicitly as:

$$H_a(t) = \sum_{i=1}^{N} \left(\omega_i a^\dagger_i a_i + f_i(t) a^\dagger_i + f^*_i(t) a_i \right) + \sum_k \omega_k c^\dagger_k c_k + \sum_{ik} \left(V_{ik} a^\dagger_i c_k + \text{H.c.} \right), \tag{61}$$

where $\omega_k = \omega_0 - 2\xi_0 \cos(k)$, and $V_{ik} = \sqrt{\frac{2}{\pi}}\, \xi_{in_i} \sin(n_i k)$. For the circuit contains a nanocavity (at the center) coupled to M individual waveguides, the corresponding Hamiltonian is

$$H_b(t) = \omega_c a^\dagger a + f(t) a^\dagger + f^*(t) a + \sum_{\alpha k} \omega_{\alpha k} c^\dagger_{\alpha k} c_{\alpha k} + \sum_{\alpha k} \left(V_{\alpha k} a^\dagger c_{\alpha k} + \text{H.c.} \right), \tag{62}$$

where the band structure of the waveguides and the coupling constants are given by Eq. (60) with $n_i = 1$. These physical realizations specify the model Hamiltonian of Eq. (14).

As an illustration, we will consider simply a nanophotonic transistor consisting of a nanocavity coupled to two coupled resonator optical waveguides (CROWs) in photonic crystals, as plotted in Fig. 2. The Hamiltonian of this simple photonic circuit is:

$$\begin{aligned} H &= \omega_c a^\dagger a + (E_0 e^{-i\omega_d t} a^\dagger + E_0 e^{i\omega_d t} a) \\ &\quad + \sum_{\alpha=1}^{2} \sum_k \omega_{\alpha k} c^\dagger_{\alpha k} c_{\alpha k} + \sum_{\alpha=1}^{2} \sum_k (V_{\alpha k} a^\dagger c_{\alpha k} + V^*_{\alpha k} a c^\dagger_{\alpha k}), \end{aligned} \tag{63}$$

where E_0 is the strength of the external driving fields in frequency ω_d. The frequency $\omega_{\alpha k}$ and the coupling constant $V_{\alpha k}$ are given by Eq. (60) with $n_i = 1$. The corresponding spectral densities are

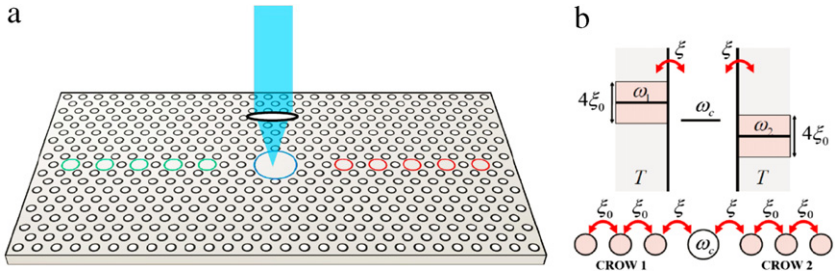

Fig. 2. (a) A nanocavity with frequency ω_c couple to two coupled resonator optical waveguides (CROWs) in photonic crystals. (b) The corresponding band structures.

given by $J_\alpha(\omega) = 2\pi g_\alpha(\omega)|V_\alpha(\omega)|^2$ where $g(\omega)$ is the density of state of the waveguide α and $V_\alpha(\omega)$ is the coupling between the cavity and the waveguide α. They can be calculated directly from Eq. (60):

$$g_\alpha(\omega) = \frac{dk}{d\omega} = \frac{1}{\sqrt{4\xi_\alpha^2 - (\omega-\omega_\alpha)^2}}, \tag{64a}$$

$$V_\alpha(\omega) = \frac{1}{\sqrt{2\pi}}\left(\frac{\xi_{c\alpha}}{\xi_\alpha}\right)\sqrt{4\xi_\alpha^2 - (\omega-\omega_\alpha)^2}, \tag{64b}$$

with $\omega_\alpha - 2\xi_\alpha < \omega < \omega_\alpha + 2\xi_\alpha$. Then the spectral density can be explicitly written as

$$J_\alpha(\omega) = \begin{cases} \eta_\alpha^2\sqrt{4\xi_\alpha^2 - (\omega-\omega_\alpha)^2}, & |\omega-\omega_\alpha| \le 2\xi_\alpha \\ 0, & |\omega-\omega_\alpha| > 2\xi_\alpha \end{cases} \tag{65}$$

with $\eta_\alpha = \xi_{c\alpha}/\xi_\alpha$. In practical, $\xi_\alpha \ll \omega_\alpha$, namely the waveguide has a very narrow band.

5.2. Analytical solutions in the weak coupling regime

First, we shall discuss the cavity photonic dynamics. Consider the case where the nanocavity is initially empty: $\langle a(t_0)\rangle = 0$ and $n(t_0) = 0$. The cavity field and the cavity photon number at a later time, i.e. Eqs. (35) and (37), become

$$\langle a(t)\rangle = y(t), \tag{66a}$$

$$n(t) = \langle a^\dagger(t)a(t)\rangle = v(t,t) + |y(t)|^2. \tag{66b}$$

Here $y(t)$ is the driving-induced field given by Eq. (29b) and $v(t,t)$ is the photon correlation due to the thermal fluctuation of the waveguides, given by Eq. (29c). Only at zero temperature, we have $v(t,t) = 0$. Then the cavity photon number equals to the absolute square of the cavity field, i.e. $n(t) = |\langle a(t)\rangle|^2$.

To see the dynamics of cavity field controlled through the driving field, we shall consider first the cavity decoupled to waveguides, i.e. $\xi_{1c} = \xi_{2c} = 0$. In this situation, the photonic propagating function in the cavity is simply given by $u(t,t_0) = e^{-i\omega_c(t-t_0)}$ and the photon correlation function $v(t,t) = 0$. Then, the cavity field and cavity photon number equal to $y(t)$ and $|y(t)|^2$, respectively, with

$$y(t) = \begin{cases} \dfrac{E_0}{\omega_d - \omega_c}[e^{-i\omega_d(t-t_0)} - e^{-i\omega_c(t-t_0)}] & \omega_d \neq \omega_c \\ E_0(t-t_0)e^{-i(\omega_c(t-t_0)+\frac{\pi}{2})} & \omega_d = \omega_c. \end{cases} \tag{67}$$

It shows that the cavity field is a coherent superposition of the cavity mode with the external driving field. If the driving field frequency differs from the cavity mode, the interference between the cavity mode and the driving field causing the photons jump in and out of the cavity with the Rabi frequency $(\omega_d - \omega_c)/2$. When the driving field is in resonance with the cavity mode, the driving field would be

completely absorbed into the cavity, and the cavity field amplitude increases linearly in time without an interference oscillation.

When the cavity couples to waveguides, generally it is not easy to find the analytical solution for $u(t,t_0)$ and $v(t,t)$. One has to solve Eqs. (28b) and (29c) numerically to understand the photonic dynamics of the driven cavity. However, in the weak coupling regime, the memory effect is negligible so that the Born–Markov approximation can be applied [22]. Then the photonic propagating function and the correlation function in weak coupling limit can be approximated (see the Appendix) by

$$u(t,t_0) \simeq e^{-(i\omega_c'+\kappa)(t-t_0)}, \tag{68a}$$

$$v(t,t) \simeq \bar{n}(\omega_c',T)[1-e^{-2\kappa(t-t_0)}], \tag{68b}$$

where $\omega_c' = \omega_c + \sum_\alpha \delta\omega_\alpha$ is a renormalized cavity frequency with frequency shift $\delta\omega_\alpha = \mathcal{P}\left[\int \frac{d\omega}{2\pi} \frac{J_\alpha(\omega)}{\omega_c-\omega}\right]$. The damping rate $\kappa = \sum_\alpha \kappa_\alpha$ with $\kappa_\alpha = J_\alpha(\omega_c)/2$ and the average photon number of the two waveguides $\bar{n}(\omega_c',T) = \sum_\alpha J_\alpha(\omega_c')n_\alpha(\omega_c')/2\kappa$.

On the other hand, to solve the driving-induced field $y(t)$ in the BM limit, special care needs to be taken since the driving field has its own character frequency ω_d which is usually different from the cavity mode frequency ω_c. Therefore, instead of applying directly the BM solution of Eq. (68a) into Eq. (29b), we have to use different character frequencies ω_c and ω_d for the homogeneous and inhomogeneous solutions of Eq. (28d) to find the BM limit of the driving-induced field $y(t)$. The detailed derivation is also given in the Appendix. The result is nontrivial:

$$y(t) \simeq \frac{E_0\exp(-i\phi)}{\sqrt{(\omega_d-\tilde{\omega}_c)^2+\tilde{\kappa}^2}}[e^{-i\omega_d(t-t_0)} - e^{-(i\omega_c'+\kappa)(t-t_0)}], \tag{69}$$

where $\phi = \tan^{-1}\frac{\tilde{\kappa}}{\omega_d-\tilde{\omega}_c}$, $\tilde{\omega}_c = \omega_c + \sum_{\alpha=1}^2 \delta\tilde{\omega}_\alpha$ with the driving field induced frequency shift $\delta\tilde{\omega}_\alpha = \mathcal{P}\int_0^\infty \frac{d\omega}{2\pi}\frac{J_\alpha(\omega)}{\omega_d-\omega}$. $\tilde{\kappa} = \sum_{\alpha=1}^2 \tilde{\kappa}_\alpha$ with $\tilde{\kappa}_\alpha = J_\alpha(\omega_d)/2$, located at the driving frequency rather than the cavity frequency. Correspondingly, the cavity field and the cavity photon number of Eq. (66) in the BM limit become

$$\langle a(t)\rangle \simeq \frac{E_0\exp(-i\phi)}{\sqrt{(\omega_d-\tilde{\omega}_c)^2+\tilde{\kappa}^2}}[e^{-i\omega_d(t-t_0)} - e^{-(i\omega_c'+\kappa)(t-t_0)}], \tag{70a}$$

$$\begin{aligned} n(t) \;\simeq\; & \bar{n}(\omega_c',T)[1-e^{-2\kappa(t-t_0)}] + \frac{E_0^2}{(\omega_d-\tilde{\omega}_c)^2+\tilde{\kappa}^2}\left[1+e^{-2\kappa(t-t_0)}\right. \\ & \left. -\; 2e^{-\kappa(t-t_0)}\cos[(\omega_d-\omega_c')(t-t_0)]\right]. \end{aligned} \tag{70b}$$

As one see, the cavity field is a coherent superposition of the external driving field and the damped cavity mode, where the damping comes from the coupling of the cavity with waveguides that induces photon dissipation from the cavity into waveguides. This damping (dissipation) effect leads cavity mode to vanish in the steady limit. Only the driving field is remained in the cavity with a modified (amplified) field amplitude $E_0' = \frac{E_0}{\sqrt{(\omega_d-\tilde{\omega}_c)^2+\tilde{\kappa}^2}}$ and a phase shift ϕ, as a feed-back effect from the coupling of the cavity with waveguides. The photon number in the cavity is then a combination of the driving-induced field plus a background noise from the thermal fluctuation of waveguides $[\sim\bar{n}(\omega_c',T)]$. These analytical results help us to understand the driven cavity dynamics in the strong coupling regime. The corresponding numerical solution will be presented later.

Furthermore, the transport phenomena of photons flowing into the waveguides can be specified by the photocurrent which can be simplified as well in the weak coupling limit:

$$\begin{aligned} I_\alpha(t) \;=\; & -2\kappa_\alpha\bar{n}(\omega_c')e^{-2\kappa(t-t_0)} + \frac{2E_0^2\kappa_\alpha}{(\tilde{\omega}_c-\omega_d)^2+\tilde{\kappa}^2} \\ & \times\left\{\frac{\tilde{\kappa}_\alpha}{\kappa_\alpha} + e^{-2\kappa(t-t_0)} - \left(1+\frac{\tilde{\kappa}_\alpha}{\kappa_\alpha}\right)e^{-\kappa(t-t_0)}\cos[(\omega_d-\omega_c')(t-t_0)]\right. \\ & \left. +\; \frac{\delta\omega_\alpha-\delta\tilde{\omega}_\alpha}{\kappa_\alpha}e^{-\kappa(t-t_0)}\sin[(\omega_d-\omega_c')(t-t_0)]\right\}. \end{aligned} \tag{71}$$

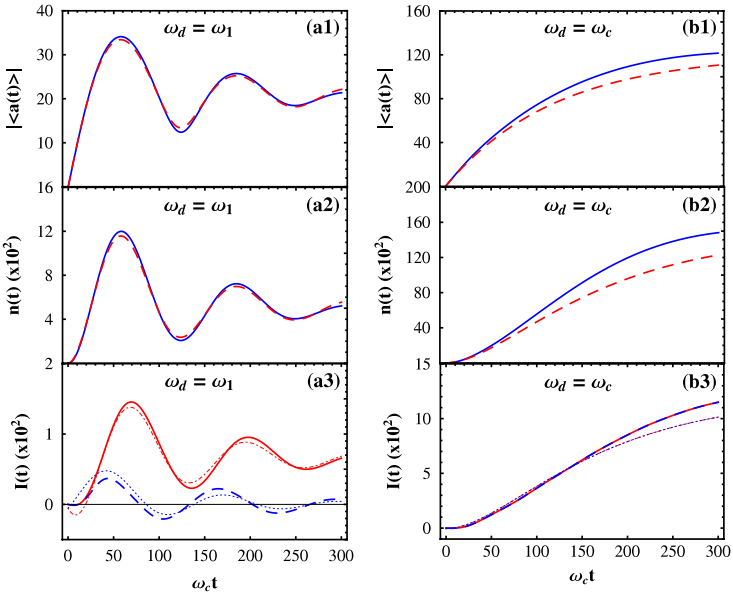

Fig. 3. Comparison of the analytical solution in the weak coupling limit with the exact numerical solution at the coupling rate $\eta = \xi/\xi_0 = 0.5$ with different driving frequency. (a1)–(a1) and (a2)–(b2) are the cavity field amplitude and cavity photon number, respectively, with the BM solution (red dashed line) and the exact solution (blue solid line). (a3)–(b3) are the photocurrent $I_1(t)$ and $I_2(t)$ with the exact solution (red solid line and blue dashed line) and the BM solution (blue dotted line and red dotted–dashed line). (For interpretation of the references to colour in this figure legend, the reader is referred to the web version of this article.)

The first term in Eq. (71) is the contribution of the waveguide thermal fluctuation, which would be vanish when the cavity is equilibrated with the waveguides. The remainders come from the response of the waveguides to the external driving field through the cavity, in which the first decay term is due to the dissipation of the cavity mode, the second and third decay terms are the thermal-fluctuation-induced decoherence (noise) of the cavity field. These three contributions together with the thermal-fluctuation-induced current (the first term) will vanish in the steady limit. The time-independent term in Eq. (71) is the steady photocurrent, which is determined by the cavity mode, the driving field frequency and the spectrum of the waveguide. When the driving field frequency lies outside the band of the waveguide α, the steady photocurrent vanishes because $\tilde{\kappa}_\alpha = J_\alpha(\omega_d)/2 = 0$. On the other hand, the photocurrent flowing into the waveguide α becomes maximal when the driving field frequency lies at the band center of the waveguide α, i.e. $\omega_d = \omega_\alpha$, see Eq. (65). This result shows that the nontrivial Born–Markovian solution in the presence of external driving field gives already a clear picture on the controllability of photonic transport in the photonic circuit through the external driving frequency.

5.3. Exact numerical solutions in both the weak and strong coupling regimes

Now, we turn to the exact numerical calculation for arbitrary coupling between the cavity and the waveguides. We will focus on the situation where the frequency of the cavity lies between the band centers of two waveguides, i.e. $\omega_c = (\omega_1+\omega_2)/2$. In the numerical calculation, we take $\omega_1 = 9.5$ GHz, $\omega_2 = 10.5$ GHz, $\xi_1 = \xi_2 = \xi = 0.3$ GHz, $\xi_{1c} = \xi_{2c} = \xi_c$, and $E_0 = 10$ GHz. We should first compare the above analytical BM solution in the weak coupling limit with the exact numerical solution of the cavity field amplitude, the cavity photon number and the photocurrent, given by Eqs. (70) and (71) and Eqs. (66) and (50), respectively. The result is plotted in Fig. 3 where the coupling rate $\eta = \xi/\xi_0 = 0.5$ which belongs to a weak coupling and the BM approximation is applicable as we have shown in [23]. From Fig. 3, we see that in the weak coupling limit, the BM solution is in good agreement with the

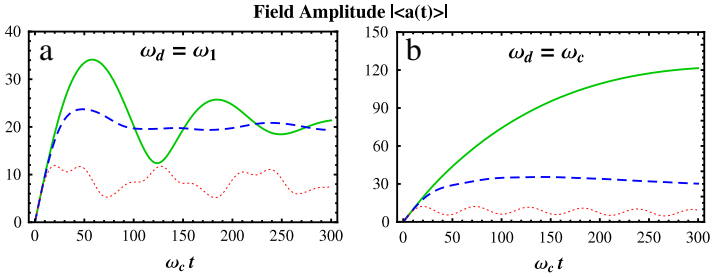

Fig. 4. The time evolution of the cavity field amplitude with different coupling strengths: $\eta = 0.5$ (solid green line), 1.0 (dashed blue line) and 2.0 (dotted red line). (a) The driving field frequency equals to the band center of the waveguide 1. (b) The driving field frequency is in resonance to the cavity mode. (For interpretation of the references to colour in this figure legend, the reader is referred to the web version of this article.)

exact solution, in particular when the driving frequency $\omega_d = \omega_1$. When the driving frequency equals to the cavity mode frequency, the deviation between the exact solution and the BM solution becomes relatively large in the steady limit. This can be seen from Eq. (70) where the amplified cavity field amplitude in the BM limit, $E_0' = \frac{E_0}{\sqrt{\delta\tilde{\omega}_c^2 + \tilde{\kappa}^2}}$, becomes sensitive to the approximation. But the qualitative behavior of the BM solution is still in good agreement with the exact solution.

Next, we shall present the exact numerical solutions for different values of the coupling constants between the cavity and the waveguides, to examine the different photonic transport dynamics in the weak coupling as well as in the strong coupling regime. Fig. 4 shows the cavity field amplitude of Eq. (66) with different coupling strengths and different driving field frequencies. Fig. 4(a) and (b) correspond to the cases of the driving frequency being in resonance with the band center of the waveguide 1 and the cavity mode, respectively. Different curves in each plot correspond to different coupling strengths between the cavity and waveguides. In the weak coupling regime, the behavior of the cavity field amplitude highly depends on the driving field frequency. When the driving field is not in resonance to the cavity mode, the field amplitude oscillates (as a result of the superposition of the driving field with the cavity mode) and decay (due to the dissipation induced by the coupling of the cavity with waveguides). When the driving field is in resonance to the cavity mode ($\omega_d = \omega_c$), the field amplitude increases gradually without oscillation. These numerical results agree with the BM solution of Eq. (70a), as shown in Fig. 3. In the strong coupling regime, the field amplitude keep oscillating without decay in both cases. The absence of the damping (dissipation) is totally due to the non-Markovian memory effect, as we have pointed out recently [22,23]. The complicated oscillating behavior (dotted red curve) in Fig. 4(a) is an interference effect between the driving field and the cavity mode with $\omega_d \neq \omega_c$. Only in the resonance case ($\omega_d = \omega_c$), the cavity field becomes coherent with the external driving field, as shown by the dotted red curve in Fig. 4(b).

Fig. 5 shows the thermal fluctuation $v(t, t)$ and the average photon number $n(t)$ in the driven cavity for different coupling strengths, different driving field frequencies and different initial temperatures. According to Eq. (66b), when the cavity is empty initially, the average cavity photon number is fully determined by the driving-induced field $|y(t)|^2$ and the thermal fluctuation induced correlation $v(t, t)$. As shown in Fig. 5, $v(t, t)$ almost equals to zero when $T = 5$ mK. In this case, $n(t) = |\langle a(t)\rangle|^2 \simeq |y(t)|^2$, namely, the cavity field is a pure coherent field induced by the external driving field. When the temperature increases, the contribution of $v(t, t)$ is increased as well. At $T = 5$ K, the contribution from the thermal fluctuation is still very small in the weak coupling, in comparison with the contribution from the driving-induced field $y(t)$. However, $v(t, t)$ becomes comparable with $y(t)$ in the strong coupling, as shows in Fig. 5(a3)–(b3). With further increase of the temperature, thermal fluctuation would destroy the coherence of the cavity field if the driving field is weak.

Fig. 6 shows the photocurrents $I_1(t)$ and $I_2(t)$ flowing from the cavity into the waveguides in different driving frequencies and coupling strengths. The frequency of the external driving field is the crucial factor for the control of the photocurrents. When the external driving field is in resonance to the cavity field, the photocurrents flowing through the waveguide 1 and the waveguide 2 are equal because of the symmetric configuration, as shown in Fig. 6(a2)–(c2). However, when the driving

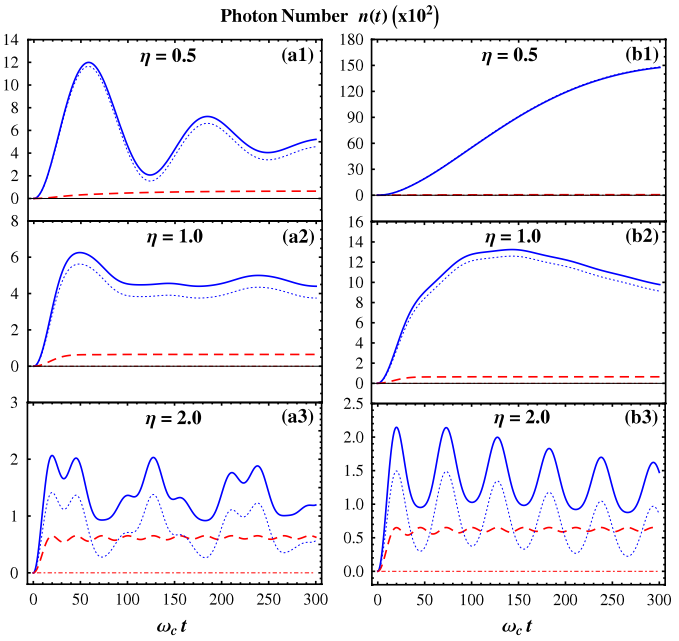

Fig. 5. The time evolution of the thermal fluctuation $v(t, t)$ (red dashed and dotted–dashed curves) and the cavity intensity (blue solid and dotted curves) at different initial temperature ($T = 5$ K and $T = 5$ mK) with different coupling strength. The left plots correspond to $\omega_d = \omega_1$ and the right plots for $\omega_d = \omega_c$. (For interpretation of the references to colour in this figure legend, the reader is referred to the web version of this article.)

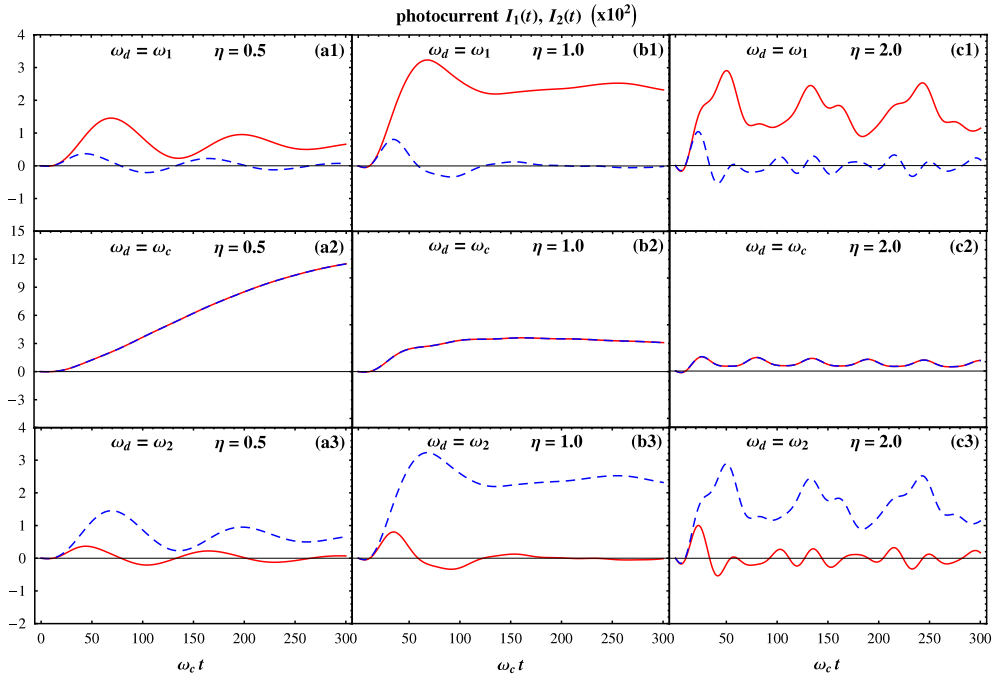

Fig. 6. Photocurrent $I_1(t)$ (solid red line) and $I_2(t)$ (dashed blue line) in different coupling strength and driving frequencies. Here, the initial temperature $T = 5$ K. (For interpretation of the references to colour in this figure legend, the reader is referred to the web version of this article.)

field is in resonance to the band center of the waveguide 1, the photocurrent $I_1(t)$ flowing through the waveguide 1 is dominated while the photocurrent $I_2(t)$ flowing through the waveguide 2 is suppressed, see Fig. 6(a1)–(c1). Similarly, when the driving field is in resonance to the band center of the waveguide 2, the photocurrent $I_2(t)$ becomes dominated and the photocurrent $I_1(t)$ is suppressed, as shown by Fig. 6(a3)–(c3). These results explicitly demonstrate the controllability of the photonic quantum transport through the driven cavity.

The above numerical analysis show that photonic dynamics and photonic transport in an all-optical circuit can be manipulated efficiently through the external driving signals and the internal cavity-waveguide couplings. Photon dissipation and thermal fluctuation appear in all the cases. In weak coupling limit, the cavity mode will decay so that only the driving-induced field plays the role in the photonic transport. The strong coupling between the cavity and the waveguides can largely suppress the cavity photon dissipation, due to the non-Markovian memory effect. In this case, the cavity mode can serve as a new control field in the photonic transport. The photonic thermal fluctuation can be suppressed by either lowing the temperature or raising the working frequency of the device. These general properties provide a theoretical basis for the further development of integrated quantum photonic circuits.

6. Summary and prospection

In summary, we have established a quantum dissipative transport theory for nanophotonics. We mainly deal with the on-chip nanophotonic circuits which consist of all-optical integrated circuits incorporating photonic bandgap waveguides and driven resonators in photonic crystals. The transient transport of photons in nanophotonic devices is controlled through the driven resonators.

First, the photonic dynamics of the driven resonators is described with the exact master equation derived by treating the waveguides as environment, and the back-reactions between waveguides and resonators are fully accounted. The photocurrents flowing from the resonators into the waveguides, which determine the photonic transport in the circuit, are obtained directly from the master equation. This theory can be applied to photonic transport in nanophotonic devices involving single photon as well as many photons.

Second, we have shown that there exists several crucial differences between photonic transport in all-optical circuit and electronic transport in mesoscopic device. Instead of applying bias and gate voltage to control electron transport in electronic devices, the photonic transport is manipulated through external driving fields applied to waveguides or resonators. Differing from the electron transport, where the bias and gate voltages controls are embedded into the spectra, the energy levels of the system, and the coupling strength between the system and leads, the external driving fields applied to waveguides and resonators turn out to be the modified driving fields acting explicitly on the resonators, as shown in the master equation of Eq. (32). The resulting lesser Green function (Eq. (55)), thereby the photocurrent (Eq. (56)), contains additional terms induced from the external driving fields. This shows that the manipulations of photonic transport through external fields behave significantly different from those of electronic transport. In addition, the initial state dependence of the formulation also allows us to examine explicitly the non-Markovian phenomena in transient quantum transport.

Third, as a simple illustration of the theory, we investigate the photonic transport dynamics of the driven nanocavity coupled to two waveguides. The cavity field coherence, the cavity intensity, as well as the photocurrents flowing into the waveguides are solved analytically in the weak coupling limit. Numerically exact calculations are also given for strong couplings regime with different driving frequencies. Non-Markovian memory effects in the strong coupling regime are manifested. The thermal fluctuation that affects to coherent property of the cavity field is also demonstrated. The analytical and numerical results show the controllability for the wavelength-selective quantum transport. The efficient controllability together with the simplicity of the implementation of the photonic circuit in photonic crystals provide potential applications in the integrated quantum photonic circuitry.

Finally, it should also be pointed out that the present theory can be directly extended to the investigation of various photonic transport phenomena in other nanoscale photonic metamaterials [56] and phononic transport in nanoscale heat-conducting systems [57]. The present theory

incorporates the Feynman–Vernon influence functional approach with Keldysh's nonequilibrium Green function technique, which makes it more powerful in the study of nonequilibrium dynamics for open quantum systems. The generalization of the present theory to nonequilibrium dynamics of ultracold atomic Bose–Einstein condensation is in progress. Various novel nanodevices, such as photon entanglement through photonic crystal waveguides [58,59], can be designed with the help of the present theory. And more applications will be presented in future works.

Acknowledgments

This work is supported by the National Science Council of ROC under Contract No. NSC-99-2112-M-006-008-MY3. We also acknowledge the support from the National Center for Theoretical Science of Taiwan. WMZ would also like to thank the National University of Singapore for the warm hospitality during his visit.

Appendix. Analytical solutions in the weak coupling limit with external driving field

In this appendix, we shall present analytical solutions in the weak coupling limit for the photonic circuit given in Section 5. First, let us solve the photon propagating function $u(t, t_0)$. To do so, let $u(t, t_0) \equiv e^{-i\omega_c(t-t_0)}A(t)$. Then Eq. (28a) is reduced to

$$\frac{dA(t)}{dt} + \int_0^{t-t_0} dt' \mathbf{g}(t') e^{i\omega_c t'} A(t-t') = 0. \tag{72}$$

When the spectrum of the waveguides are broad enough and the coupling between the waveguides and the system is weak, the memory effect between the system and the reservoir can be ignored so that the Markov limit is reached. In other words, $A(t-\tau)$ in the integration can be replaced by $A(t)$ and the integration time t' can be considered much shorter in comparison with the character time t of the cavity field [45]. Then,

$$\int_0^{t-t_0} dt' \mathbf{g}(t') e^{i\omega_c t'} A(t-t') \simeq \left[\lim_{t\to\infty} \int_0^{t-t_0} dt' \mathbf{g}(t') e^{i\omega_c t'}\right] A(t) = (i\delta\omega_c + \kappa) A(t), \tag{73}$$

where $\delta\omega_c = \sum_{\alpha=1}^{2} \delta\omega_\alpha$ is the cavity frequency shift with $\delta\omega_\alpha = \mathcal{P}\int_0^\infty \frac{d\omega}{2\pi} \frac{J_\alpha(\omega)}{\omega_c - \omega}$. The cavity damping rate $\kappa = \sum_{\alpha=1}^{2} \kappa_\alpha$ with $\kappa_\alpha = J_\alpha(\omega_c)/2$. Thus, the photonic propagating function is approximated analytically by

$$u(t, t_0) \simeq e^{-(i\omega_c' + \kappa)(t-t_0)}, \tag{74}$$

and the renormalized cavity frequency $\omega_c' = \omega_c + \delta\omega_c$.

Next, we shall solve the correlation function $v(t, t)$ in the same approximation. Note that $\frac{v(t,t)}{dt} \neq \frac{v(\tau,t)}{d\tau}|_{\tau=t}$, one should not directly use Eq. (28c) to solve $v(t, t)$. It is more convenient to take the time derivative of the solution $v(t, t)$ given by (29c) and utilize the Eq. (28a), which leads to

$$\frac{v(t,t)}{dt} + 2\mathrm{Re}\int_{t_0}^{t} d\tau \mathbf{g}(t-\tau) v(\tau, t) = 2\mathrm{Re}\int_{t_0}^{t} d\tau \tilde{\mathbf{g}}(t-\tau) \bar{u}(\tau, t). \tag{75}$$

Then using the same approximation of Eq. (73), we have

$$\begin{aligned} &\mathrm{Re}\int_{t_0}^{t} d\tau \mathbf{g}(t-\tau) v(\tau, t) \simeq \mathrm{Re}\int_{t_0}^{t} d\tau g(t-\tau) e^{i\omega_c(t-\tau)} v(t, t) \simeq \kappa v(t, t), \\ &\mathrm{Re}\int_{t_0}^{t} d\tau \tilde{\mathbf{g}}(t-\tau) \bar{u}(\tau, t) \simeq \mathrm{Re}\int_{t_0}^{t} d\tau \tilde{g}(t-\tau) e^{i\omega_c'(t-\tau)} \simeq \sum_{\alpha=1}^{2} J_\alpha(\omega_c') n_\alpha(\omega_c'). \end{aligned} \tag{76}$$

The solution of Eq. (75) is then approximately given by

$$v(t,t) \simeq \bar{n}(\omega_c', T)[1 - e^{-2\kappa(t-t_0)}], \tag{77}$$

where $\bar{n}(\omega_c', T) = \sum_{\alpha=1}^{2} n_\alpha(\omega_c') J_\alpha(\omega_c')/2\kappa$. The analytical solutions of Eqs. (74) and (77) are the well-known Born–Markov limit of the cavity field coupled to a thermal bath.

With the external driving field $f(t) = E_0 e^{-i\omega_d(t-t_0)}$ being explicitly added, the equation of motion for the driving-induced field $y(\tau)$ becomes:

$$\frac{dy(t)}{dt} + i\omega_c y(t) + \int_{t_0}^{t} d\tau g(t-\tau) y(\tau) = -iE_0 e^{-i\omega_d(t-t_0)}. \tag{78}$$

The homogeneous solution of this equation is just $u(\tau, t_0)$ with the character frequency ω_c, whose BM limit solution has been given by Eq. (74). The inhomogeneous solution of $y(t)$ must have a form $Be^{-i\omega_d(t-t_0)}$, where B is a constant and ω_d is the character frequency. In the BM limit, using the same approximation but noting the different character frequency, we find that

$$B = \frac{E_0 \exp(-i\phi)}{\sqrt{(\omega_d - \tilde{\omega}_c)^2 + \tilde{\kappa}^2}}, \tag{79}$$

where $\phi = \tan^{-1} \frac{\kappa}{\omega_d - \tilde{\omega}_c}$, $\tilde{\omega}_c = \omega_c + \sum_{\alpha=1}^{2} \delta\tilde{\omega}_\alpha$ with the driving field induced frequency shift $\delta\tilde{\omega}_\alpha = \mathcal{P}\int_0^\infty \frac{d\omega}{2\pi} \frac{J_\alpha(\omega)}{\omega_d - \omega}$ and $\tilde{\kappa} = \sum_{\alpha=1}^{2} \tilde{\kappa}_\alpha$ with $\tilde{\kappa}_\alpha = J_\alpha(\omega_d)/2$. Put the homogeneous solution and the inhomogeneous solution together with the initial condition $y(t_0) = 0$, we obtain the driving-induced field in the BM limit:

$$y(t) \simeq \frac{E_0 \exp(-i\phi)}{\sqrt{(\omega_d - \tilde{\omega}_c)^2 + \tilde{\kappa}^2}} \left[e^{-i\omega_d(t-t_0)} - e^{-(i\omega_c' + \kappa)(t-t_0)} \right]. \tag{80}$$

From the above solution for the propagating function $u(\tau, t_0)$, the correlation function $v(t,t)$ and the driving-induced field $y(t)$, it is easy to find analytically the cavity field and the cavity photon number in the BM limit, i.e. Eq. (70). Utilizing the similar approximation in the above derivation, the photocurrent flowing through the waveguide $\alpha = 1, 2$ in the BM limit are given by Eq. (71). Furthermore, we can also find the source term in Eq. (51) in the BM limit by substituting the BM solution of the cavity field, Eq. (70a), into Eq. (46a):

$$S(t) = \frac{2\tilde{\kappa} E_0^2}{(\omega_d - \tilde{\omega}_c)^2 + \tilde{\kappa}^2} \left\{ 1 + e^{-\kappa(t-t_0)} \cos[(\omega_d - \omega_c')(t-t_0)] + \frac{\omega_d - \tilde{\omega}_c}{\tilde{\kappa}} e^{-\kappa(t-t_0)} \sin[(\omega_d - \omega_c')(t-t_0)] \right\}. \tag{81}$$

As a self-consistent check, the BM solutions of the cavity photon number, the driving source and the photocurrent flowing into waveguides satisfy the quantum continuous equation:

$$\frac{dn(t)}{dt} = S(t) - \sum_{\alpha=1}^{2} I_\alpha(t). \tag{82}$$

References

[1] J.D. Joannoupoulos, S.G. Johnson, J.W. Winn, R.D. Meade, Photonic Crystals: Modeling the Flow of Light, Princeton, New York, 2008.
[2] M. Notomi, Rep. Progr. Phys. 73 (2010) 096501.
[3] S. Noda, A. Chutinan, M. Imada, Nature 407 (2000) 608;
Y. Akahane, T. Asano, B.S. Song, S. Noda, Nature 425 (2003) 944.
[4] H. Gersen, T.J. Karle, R.J.P. Engelen, W. Bogaerts, J.P. Korterik, N.F. van Hulst, T.F. Krauss, L. Kuipers1, Phys. Rev. Lett. 94 (2005) 073903;
T. Baba, Nat. Photon. 2 (2008) 465;
R.M. De La Rue, Nat. Photon. 2 (2008) 715.
[5] A. Yariv, Y. Xu, R.K. Lee, A. Scherer, Opt. Lett. 24 (1999) 711;
M. Bayindir, B. Temelkuran, E. Ozbay, Phys. Rev. Lett. 84 (2000) 2140.
[6] K. Nozaki, T. Tanabe, A. Shinya, S. Matsuo, T. Sato, H. Taniyama, M. Notomi, Nat. Photon. 4 (2010) 477.

[7] S.H. Fan, P.R. Villeneuve, J.D. Joannopoulos, Opt. Express 3 (1998) 4;
H.G. Park, C.J. Barrelet, Y. Wu, B. Ting, F. Qian, C.M. Lieber, Nat. Photon. 2 (2008) 622.
[8] T. Baba, Nat. Photon. 1 (2007) 11;
Q. Xu, P. Dong, M. Lipson, Nat. Phys. 3 (2007) 406.
[9] V.S.C. Manga Rao, S. Hughes, Phys. Rev. Lett. 99 (2007) 193901.
[10] W. Yuan, L. Wei, T.T. Alkeskjold, A. Bjarklev, O. Bang, Opt. Express 17 (2009) 19356;
D.J.J. Hua, P. Shum, C. Lu, X.W. Sun, G.B. Ren, X. Yu, G.H. Wang, Opt. Commun. 282 (2009) 2343.
[11] F. Du, Y.Q. Lu, S.T. Wu, Appl. Phys. Lett. 85 (2004) 2181;
N. Malkova, C.Z. Ning, J. Opt. Soc. Am. B 23 (2006) 978.
[12] D. Psaltis, S.R. Quake, C. Yang, Nature 442 (2006) 381;
C. Monat, P. Domachuk, B.J. Eggleton, Nat. Photon. 1 (2007) 106;
L. Scolari, S. Gauza, H. Xianyu, L. Zhai, L. Eskildsen, T.T. Alkeskjold, S.T. Wu, A. Bjarklev, Opt. Express 17 (2009) 3754.
[13] W. Park, J.B. Lee, Appl. Phys. Lett. 85 (2004) 4845.
[14] Y. Kanamori, K. Takahashi, K. Hane, Appl. Phys. Lett. 95 (2009) 171911;
X.Y. Chew, G.Y. Zhou, F.S. Chau, J. Deng, X.S. Tang, Y.C. Loke, Opt. Lett. 35 (2010) 2517.
[15] P. Lambropoulos, G. Nikolopoulos, T.R. Nielsen, S. Bay, Rep. Progr. Phys. 63 (2000) 455.
[16] D. Mogilevtsev, S. Kilin, Progr. Opt. 54 (2010) 89–148.
[17] E. Yablonovitch, Phys. Rev. Lett. 58 (1987) 2059;
S. John, Phys. Rev. Lett. 58 (1987) 2486.
[18] S. John, J. Wang, Phys. Rev. Lett. 64 (1990) 2418; Phys. Rev. B 43 (1991) 12 772;
S. John, T. Quang, Phys. Rev. A 50 (1994) 1764.
[19] S. Kilin, D. Mogilevtsev, Laser Phys. 2 (1992) 153.
[20] A.G. Kofman, G. Kurizki, B. Sherman, J. Mod. Opt. 41 (1994) 353.
[21] T. Quang, M. Woldeyohannes, S. John, G.S. Agarwal, Phys. Rev. Lett. 79 (1997) 5238;
S. John, T. Quang, Phys. Rev. Lett. 78 (1997) 1888;
M. Florescu, S. John, Phys. Rev. A 64 (2001) 033801.
[22] H.N. Xiong, W.M. Zhang, X. Wang, M.H. Wu, Phys. Rev. A 82 (2010) 012105.
[23] M.H. Wu, C.U. Lei, W.M. Zhang, H.N. Xiong, Opt. Express 18 (2010) 18407;
C.U. Lei, W.M. Zhang, Phys. Rev. A 84 (2011) 214304.
[24] J. Schwinger, J. Math. Phys. 2 (1961) 407;
L.V. Keldysh, Sov. Phys. JETP 20 (1965) 1018.
[25] L.P. Kadanoff, G. Baym, Quantum Statistical Mechanics, Benjamin, New York, 1962.
[26] R.P. Feynman, F.L. Vernon, Ann. Phys. 24 (1963) 118.
[27] K.C. Chou, Z.B. Su, B.L. Hao, L. Yu, Phys. Rep. 118 (1985) 1.
[28] W.M. Zhang, L. Wilets, Phys. Rev. C 45 (1992) 1900.
[29] H. Haug, A.P. Jauho, Quantum Kinetics in Transport and Optics of Semiconductors, second ed., in: Springer Series in Solid-State Sciences, vol. 123, Springer-Verlag, Berlin, 2008.
[30] A.J. Leggett, S. Chakravarty, A.T. Dorsey, M.P. Fisher, A. Garg, W. Zwerger, Rev. Modern Phys. 59 (1987) 1.
[31] W.H. Zurek, Phys. Today 44 (10) (1991) 36; Rev. Modern Phys. 75 (2003) 715.
[32] A.O. Caldeira, A.J. Leggett, Physica A 121 (1983) 587.
[33] B.L. Hu, J.P. Paz, Y.H. Zhang, Phys. Rev. D 45 (1992) 2843.
[34] U. Weiss, Quantum Dissipative Systems, third ed., World Scientific, Singapore, 2008.
[35] H.-P. Breuer, F. Petruccione, The Theory of Open Quantum Systems, Oxford University Press, Oxford, 2002.
[36] H. Schoeller, G. Schön, Phys. Rev. B 50 (1994) 18436.
[37] J.S. Jin, X. Zheng, Y.J. Yan, J. Chem. Phys. 128 (2008) 234703.
[38] M.W.Y. Tu, W.M. Zhang, Phys. Rev. B 78 (2008) 235311.
[39] J.S. Jin, M.W.Y. Tu, W.M. Zhang, Y.J. Yan, New J. Phys. 12 (2010) 083013.
[40] C. Viviescas, G. Hackenbroich, Phys. Rev. A 67 (2003) 013805.
[41] R.J. Glaber, M. Lewenstein, Phys. Rev. A 43 (1991) 467.
[42] H. Feshbach, Ann. Phys. 19 (1962) 287–313.
[43] H.J. Carmichael, An Open Systems Approach to Quantum Optics, in: Lecture Notes in Physics, vol. m18, Springer-Verlag, Berlin, 1993.
[44] W.M. Zhang, D.H. Feng, R. Gilmore, Rev. Modern Phys. 62 (1990) 867.
[45] J.H. An, W.M. Zhang, Phys. Rev. A 76 (2007) 042127;
J.H. An, M. Feng, W.M. Zhang, Quantum Inf. Comput. 9 (2009) 0317.
[46] Usually the stationary path (or stationary phase) method is an approximation to path integral calculations. When the path integrals can be reduced to Gaussian integrals, the stationary path method will lead to an exact solution. For more detailed discussion, see R.P. Feynman, A.R. Hibbs, Quantum Mechanics and Path Integrals, McGraw-Hill, 1965.
[47] G. Lindblad, Comm. Math. Phys. 48 (1976) 119;
V. Gorini, A. Kossakowski, E.C.G. Sudarshan, J. Math. Phys. 17 (1976) 821.
[48] R. Alicki, K. Lendi, Quantum Dynamical Semigroups and Applications, in: Lecture Notes in Physics, Springer-Verlag, Berlin, 1987.
[49] R. Karrlein, H. Grabert, Phys. Rev. E 55 (1997) 153.
[50] F. Haake, R. Reibold, Phys. Rev. A 32 (1985) 2462;
J.J. Halliwell, T. Yu, Phys. Rev. D 53 (1996) 2012;
G.W. Ford, R.F. OConnell, Phys. Rev. D 64 (2001) 105020.
[51] T. Strunz, T. Yu, Phys. Rev. A 69 (2004) 052115.
[52] C.-H. Chou, T. Yu, B.L. Hu, Phys. Rev. E 77 (2008) 011112.
[53] J.P. Paz, A.J. Roncaglia, Phys. Rev. Lett. 100 (2008) 220401; Phys. Rev. A 79 (2009) 032102.
[54] R.X. Xu, V.L. Tian, J. Xu, Y.J. Yan, J. Chem. Phys. 130 (2009) 074107.
[55] Y. Liu, Z. Wang, M.H. Han, S.H. Fan, R. Dutton, Opt. Express 13 (2005) 4539.

[56] M. Engheta, Science 317 (2007) 1698.
[57] L. Wang, B. Li, Phys. World 21 (2008) 27;
C.R. Otey, W.T. Lau, S.H. Fan, Phys. Rev. Lett. 104 (2010) 154301.
[58] S. Hughes, Phys. Rev. Lett. 94 (2005) 227402;
S. Hughes, Phys. Rev. Lett. 98 (2007) 083606.
[59] H.T. Tan, W.M. Zhang, Phys. Rev. A 83 (2011) 062310.